Free Vibration and Thermal Analysis of Randomly Oriented Carbon Nano Tube Based Functionally Graded Beam

A THESIS SUBMITTED IN THE PARTIAL FULFILLMENT

OF THE REQUIREMENTS FOR THE DEGREE OF

Master of Technology
in
MECHANICAL ENGINEERING

[Specialization: Machine Design and Analysis]

By

Prasad K. Inamdar

(211ME1157)

DEPARTMENT OF MECHANICAL ENGINEERING

NATIONAL INSTITUTE OF TECHNOLOGY ROURKELA

YEAR 2012-2013

Free Vibration and Thermal Analysis of Randomly Oriented Carbon Nano Tube Based Functionally Graded Beam

A THESIS SUBMITTED IN THE PARTIAL FULFILLMENT

OF THE REQUIREMENTS FOR THE DEGREE OF

Master of Technology
in
MECHANICAL ENGINEERING

[Specialization: Machine Design and Analysis]

By

Prasad K. Inamdar

(211ME1157)

Under the Supervision of

Prof. T. ROY

DEPARTMENT OF MECHANICAL ENGINEERING

NATIONAL INSTITUTE OF TECHNOLOGY ROURKELA

YEAR 2012-2013

National Institute Of Technology

Rourkela

CERTIFICATE

This is to certify that the thesis entitled, "Free Vibration and Thermal Analysis of Randomly Oriented Carbon Nano Tube Based Functionally Graded Beam" submitted by Mr. Prasad K. Inamdar in partial fulfillment of the requirements for the award of MASTER OF TECHNOLOGY Degree in MECHANICAL ENGINEERING with specialization in MACHINE DESIGN AND ANALYSIS at the National Institute of Technology, Rourkela (India) is an authentic Work carried out by him under my supervision and guidance.

To the best of my knowledge, the matter embodied in the thesis has not been submitted to any other University / Institute for the award of any Degree or Diploma.

Date:

Dr. TARAPADA ROY
Department of Mechanical Engineering
National Institute of Technology
Rourkela-769008

ACKNOWLEDGEMENT

First and foremost I offer my sincerest gratitude and respect to my supervisor and guide **Dr. TARAPADA ROY**, Department of Mechanical Engineering, for his invaluable guidance and suggestions to me during my study. I consider myself extremely fortunate to have had the opportunity of associating myself with him for one year. This thesis was made possible by his patience and persistence.

After the completion of this Thesis, I experience a feeling of achievement and satisfaction. Looking into the past I realize how impossible it was for me to succeed on my own. I wish to express my deep gratitude to all those who extended their helping hands towards me in various ways during my tenure at NIT Rourkela. I greatly appreciate & convey my heartfelt thanks to my colleagues, dear ones & all those who helped me in the completion of this work. I am especially indebted to my parents for their love, sacrifice, and support. They are my first teachers after I came to this world and have set great examples for me about how to live, study and work.

I also express my sincere gratitude to Prof. (Dr.) K. P. Maity, Head of the Department, Mechanical Engineering for valuable departmental facilities.

PRASAD K. INAMDAR

Roll No: - 211ME1157

INDEX

LIST OF FIGURES

LIST OF TABLES

ABSTRACT

Modern technology demands materials having improved mechanical, thermal and chemical properties which must sustain the different environmental conditions. The carbon nanotube (CNT) reinforced functionally graded materials (FGM) are expected to be the new generation materials having wide range of unexplored potential applications in various technological areas such as aerospace, defense, energy, automobile, medical, structural and chemical industry. Present work deals with the finite element modeling and free vibration analysis of CNT based functionally graded beam using three dimensional Timoshenko beam theory. It has been assumed that the material properties of CNT based FG beam varies only along the thickness and these properties are evaluated by rule of mixture. The extended Hamilton's principle has been applied to find out the governing equations of CNT based FG beam. Finite element method is used to solve governing equation with the exact shape functions. Natural frequencies are calculated and validated with available literature. The convergence study has been carried out with obtained results. The effect of variation of CNT volume fraction and boundary conditions on the natural frequency of the beam has also been studied.

Initial analysis deals with CNTs assumed to be oriented along the length direction only. But practically it is not possible. So, further work deals with the free vibration analysis of functionally graded nano composite beams reinforced by randomly oriented straight single-walled carbon nanotubes (SWCNTs). The Eshelby–Mori–Tanaka approach based on an equivalent fiber is used to investigate the material properties of the beam. The equations of motion are derived by using Hamilton's principle. Results are presented in tabular and graphical forms to show the effects of carbon nanotube orientations, slenderness ratios and boundary conditions on the dynamic behavior of the beam.

Mainly, Functionally Graded Materials (FGMs) are invented for high temperature applications such as Aerospace and Nuclear industries. Moreover, Carbon Nano Tubes (CNTs) are reinforced with FGM to improve their thermal properties along with Mechanical and Electrical properties. So, next important work is the thermal analysis of Carbon Nano Tubes based FG (FG-CNT) Timoshenko beam. Different types of temperature distributions are used to

find out the thermal behavior of Timoshenko beam. However, the material property distribution is assumed to be exponential along the thickness direction for exponential type temperature distribution, linear and power law type material distribution for linear type temperature distribution. First order Shear Deformation Theory (FSDT) is implemented along with plain strain condition to formulate expressions for stresses and strains. Finally, effect of linear and exponential type of temperature distributions on Young's modulus, total stresses and strains is evaluated numerically for given beam. Finite difference method is also applied to find out temperature distribution for power law material distribution. Same thermal analysis is also carried out in this case also. The effect of CNT orientation on stresses and strains has also been found out for exponential distribution of material and temperature. The comparison of these cases will lead to the conclusion and it will serve the purpose of presented work.

Key words: *Functionally Graded Material; Timoshenko beam theory; Free Vibration Analysis; Randomly Oriented Carbon Nano-Tube; Thermal Analysis.*

Chapter 1
INTRODUCTION AND LAYOUT OF PRESENT WORK

1.1 INTRODUCTION

Functionally Graded Material (FGM) belongs to a class of advanced material characterized by variation in properties as the dimension varies. FGM was invented with the prime requirement of thermal stability at high temperatures along with better mechanical properties. FGM concept was originated in Japan in 1984 during the space plane project. Metallic part of FGM will take care of better mechanical properties and ceramic part will take care of thermal stability at high temperatures. The overall properties of FGM are unique and different from any of the individual material that forms it. Due to these advantages FGM has a wide range of applications such as in

- Aerospace to make space plane bodies, components of the rocket engines
- Medicine to replace the living tissues like bones and teeth
- Defence as a penetration resistant material for bullet proof vests as well as armour plates
- Energy as thermal barrier, protective blade in gas turbine
- Optoelectronics as graded refractive index material
- Other applications consist of automobile engine component and nuclear reactor components etc.

These applications explicitly require good thermal properties. So, it is important that analysis of thermal behaviour of FGM should be carried out which has initiated the work related to this area. Lot of researchers have presented their work so far.

CNTs are known to be discovered by Iijima in 1991. CNT exhibits extraordinary mechanical properties: the Young's modulus is over 1 Tera Pascal. The estimated tensile strength is 200 GPa. It is due to carbon-carbon sp^2 bonding. These properties are ideal for reinforced composites, nano electromechanical systems (NEMS). Carbon Nanotubes (CNTs) are also known for their good mechanical and electrical properties. It is good thermal conductor and also shows superconductivity. Thus the use of CNT with Functionally Graded Material (FGM) provides definitely improved mechanical, electrical as well as thermal properties. Important advantages of CNT based FGM are listed below:

1. Higher strength to density ratio
2. Higher stiffness to density ratio
3. Better fatigue and wear resistance
4. Better elevated temperature properties (Higher strength-Lower creep rate)
5. Ability to fabricate directional mechanical properties
6. Provide multi functionality
7. Provide ability to control the deformation, dynamic response of the system, wear and corrosion of parts etc.
8. Provide ability to remove stress concentrations
9. Provide opportunities to take the benefits of different material systems

The key of using CNT based FGM is that one can obtain these properties as per the requirement just by varying the distribution and composition of CNT. That's how one can get directional properties and can control other parameters. Another advantage stated above is the stress concentration free material. It is because, the cross-section shows there are no layers inside the material and instead there is a continuous gradation of materials from top to bottom. So, there is no stress concentration and delamination of layers. As it can be manufactured from CNT, polymers, ceramics, one can take the advantages of each constituent material.

CNT is a new form of carbon, configurationally equivalent to 2-D graphene sheet rolled into a tubular form. It is grown by several techniques in the laboratory which is just a few nanometers in diameter and several microns in length. Main problems facing the manufacturers are difficulty in homogeneous dispersion of CNT into the matrix material which results in low interfacial bond strength between these constituents and it affects the quality of the product. There is also a problem of mass production with low cost. To overcome these problems up to certain extent, there are different techniques to manufacture the CNT based FGM. Most common method is powder metallurgy. Besides this, there are also many methods such as melting and solidification, thermal spray including plasma and cold spraying, electrochemical deposition, vapour deposition and nano-scale dispersion. The CNT based functionally graded materials are used in wind turbines, tissue engineering, thin films of shape memory alloys, nano-electromechanical systems such as micro sensors used in robotics , micro actuators, telecommunications and transport industry.

1.2 LAYOUT OF PRESENT WORK

Present work is divided into three chapters as Free Vibration Analysis, Effect of CNT Orientation and Thermal Analysis. First chapter deals with finding out the material properties of the beam which is assumed to vary along the thickness. Later finding out the translational and kinetic energy of the Timoshenko beam, applying Hamilton's theorem to find out governing equation and solving it by using Finite element analysis to obtain equation of motion. Present theory is validated first and then effect of CNT volume fraction and slenderness ratio is obtained. Dynamic analysis is also carried to find out the displacement response. Second chapter deals with the effect of CNT orientation. Due to CNT orientation Young's modulus of the material changes which further affects the natural frequency of the system. This effect is obtained for different CNT volume fractions and slenderness ratios. Third chapter deals with thermal analysis of CNT based FG Timoshenko beam. Different types of thermal laws are applied with different material property variation to study the combined effect of thermal and material property variation on thermal stresses and strains. CNT orientation effect on the thermal stresses and strains is also obtained. Later finite difference method is applied to find out temperature distribution along the beam. That is also tested for finding out the effect of CNT orientation. The comparison between each case is presented graphically.

Finally, based on the output from each chapter conclusions are drawn which will be helpful for using CNT based FGM in practical situations.

Chapter 2
LITERATURE SURVEY

All the work that has been carried out up till is presented here regarding the properties of FGM, vibration analysis of a nano composed functionally graded material shaft using finite element modelling and thermal analysis. So, majorly it deals with material sciences, rotor dynamics, FEM, theory of vibrations, and thermodynamics. Literature survey consists of 3 parts as discussed above i.e. finding out material properties, vibration analysis and thermal analysis.

2.1 PROPERTIES OF FGM

Metals are good conductors of heat and ceramics acts as good insulators. So, they are used individually according to the requirement, but there are certain areas where both are needed simultaneously. In these applications metals and ceramics are bonded directly. At elevated temp it is found that thermal stresses are produced which is responsible for debonding of metal and ceramics as well the delamination in ceramics takes place. To avoid this, scientist Kawasaki and Watanabe proposed graded interlayer concept for metals and ceramics. Such material possesses super heat resistant property and sufficient toughness which also reduces the thermal stresses at elevated temp. This concept is known as Functionally Graded Material (FGM). [1] So, one can say FGM is a material in which mass and weight proportion is varied along the cross-section. Generally, ceramics have high percentage than metals on the outside, so that it can be used at elevated temperatures. The concept of FGM is discovered after the concept of composite materials. In case of composite materials the metal fibre is surrounded by the matrix, which gives high specific strength and stiffness with minimum specific density. In materials science "functionally graded material (FGM)" may be characterized by the variation in composition and structure gradually over volume resulting in corresponding changes in the properties of the material. The materials can be designed according to specific function and applications. Various approaches based on the bulk (particulate processing) perform processing layer processing and melt processing is used to fabricate the functionally graded materials. The basic unit for FGM representation is maxel the term maxel was introduced in 2005 by Rajeev Dwivedi and Radovan Kovacevic at Research Centre for Advanced Manufacturing (RCAM), the attributes of maxel include the location and volume fraction of individual material components.

An overview of FGM was taken by Mahamood and Akinlabi [2]. The fabrication processes, area of application, some recent research studies and the most promising FGM fabrication method (solid freeform SFF) was presented by them. The processing technique of FGM consists of vapour deposition, powder metallurgy, centrifugal and SFF. For future research, SFF method needs modification through extensive characterization so that the cost of FGM will be reduced and reliability will be increased. Durodola and Attia [3] focused mainly on FGM materials for rotating hollow and solid disks. In their paper, FGM was considered as a non-homogeneous orthotropic material. The property variation is considered as exponential. The hoop stresses and radial stresses were calculated after finding out the Young's modulus for FGM layer wise which vary along the radial direction only. Different values were obtained for different values of exponent. Aboudi and Arnold [4] considered the higher order micromechanical theory. It was more advantageous than micromechanics approach which was based on representative volume element. As RVE do not deal with continuously changing properties due to non-uniform inclusion spacing. In their paper they considered only unidirectional grading of properties. It was applied for thermal and mechanical fields in FGM. Giunta et al. [5] considered the distribution of material properties according to power law in terms of the volume fraction of the material constituents. The properties such as Young's modulus, Poisson's ratio and density vary along 1 direction and two perpendicular directions together or independently.

2.2 VIBRATION ANALYSIS OF CNT BASED FGM

The later inventions in the field of material science have proved that CNT with Functionally Graded Material (FGM) provides improved mechanical, electrical as well as thermal properties. Andrews et al. [6] fabricated the multi-walled carbon nanotube/polymer composites by shear mixing. Results showed that as concentration of nanotubes increases both strength and stiffness increases. Yas and Heshmati [7] worked on dynamics of functionally graded nano composite beams with randomly oriented single walled carbon nano tubes. They found that under the action of moving load, CNT-FGM beam with symmetrical distribution gives superior properties than that of unsymmetrical distribution. Alshorbagy et al. [8] presented the dynamic characteristics of functionally graded beam with gradation of material in axially or transversally through the thickness based on the power law. They converted geometrically non-uniform beam into axially or transversely uniform geometrical beam.

The work carried out by Liao-Long Ke et al. [9] gave the information about the nonlinear free vibration of functionally graded nano composite beams with single-walled carbon nanotubes (SWCNTs). It was based on Timoshenko beam theory and von Karman geometric nonlinearity. They also considered the gradation of material properties in thickness direction only. Khosrozadeh and Hajabasi [10] worked on free vibration of embedded double-walled carbon nanotubes considering nonlinear interlayer van der Waals forces. It was based on Euler-Bernoulli theory. The variation of the interlayer distance along the circumference of DWCNTs causes the inner and outer tubes deflections which was modelled as the interlayer van der Waal force. Natsuki et al. [11] also worked on double-walled carbon nanotubes. Ray and Batra [12] demonstrated the active control of smart structures using single-walled carbon nanotube reinforced 1-3 piezoelectric composite. Micro-mechanical analysis was carried out to find out the values of effective piezoelectric moduli. Some more about the non-linear dynamic response of nanotube-reinforced composite plates was carried out by Wang and shen [13]. The material properties were considered as function of temperature. The higher order shear deformation theory was considered along with von Karman type kinematic non linearity to find the equation of motion.

Work carried out up till was not restricted to only vibration analysis; the vibration control was also included. For safe and efficient functioning of all rotating machines, Reduction of rotor vibration is very important. Das et al. [14] worked on the vibration control and stability of the system using electromagnetic exciters. They provided suitable force of actuation which was obtained by varying the control current. The rotor shaft was modelled according to Rayleigh beam theory with viscous damping. To visualise the effect of damping, the unbalance response was plotted for controlled and uncontrolled situations. The active vibration control using fuzzy logic controllers was demonstrated by Shiraji et al. [15]. They worked on both PID controller and FLC to dampen the plate vibration. For the fuzzy inputs and outputs the designed FLC used 5 membership functions. The other method of vibration analysis is Modal analysis which was given by Kim and Lee [16]. The natural characteristics of the system such as frequency, damping and mode shapes were used to describe a structure. The modal parameters may be determined by FEA or other such methods. Mostly modal analysis is used in dynamic problem, vibration or acoustics.

2.3 THERMAL ANALYSIS

Rahini and Davoodinik [17] performed the steady state heat conduction with exponential and hyperbolic temperature distributions for FG Timoshenko beam. Material properties were assumed to vary along thickness direction only. They found that better thermal behaviour of the FG beam depends on same type of material and temperature distribution. Wang and Tian [18] implemented the FEM and Finite Difference Method (FDM) for time-dependant temperature field. Initially, temperature distribution was assumed to be a function of position and time and then basic law of heat conduction was applied. FDM along with FEM was applied to solve the first order differential equations of the system. Then the temperatures for different time and co-ordinates were calculated. Karampour [19] studied the thermal and mechanical stresses in porous and hollow sphere of FGM. He gave theoretical formulations using Legendre polynomials in Navier equations for obtaining the heat conduction equations. Stresses were calculated by Euler's differential equations. Sundararajan et al. [20] proposed the nonlinear free vibrations under thermal loading for FG plates. They assumed power law distribution of temperature dependant material properties and effect of temperature field on von Karman type nonlinear vibrations were found out. The effect of thermal shock by sudden cooling in thermal conduction analysis was performed for FGM with different rules of mixture by Olayinka et al. [21]. FGM under consideration was composed of nickel and CNT with linear, quadratic and half-order gradation of properties. The result included the thermal conductivity, specific heat and density for each layer depending upon the volume fraction of CNT.

Other important aspect of thermal analysis is buckling analysis. Some important works in this direction are presented in following paragraph. Na and Kim [22] analysed the thermal buckling of three dimensional FG beam with 18 noded solid element. Uniform and non-uniform temperature distribution was considered to find out the critical buckling temperature. Javaheri and Eslami [23] assumed higher order shear deformation theory (HSDT) for rectangular FG plate and analysed the buckling with four types of temperature distributions. Prakash et al. [24] studied the bifurcation type of buckling of FG skew plates under uniform temperature field. Effective material properties were calculated by Mori-Tanaka method which varies along the thickness only. Effect of temperature distribution, skew angle aspect ratio and boundary conditions were found out on post-buckling path. Shen [25] presented the post-buckling analysis for simply supported beam for parabolic

temperature distribution and heat conduction. Material properties were assumed to be temperature dependant and follow the power law. Finally, buckling temperature and post-buckling equilibrium paths were obtained for given temperature distributions. Addition to his work, Shen [26] also presented the post-buckling analysis for axially loaded FG cylindrical shell subjected to thermal loads. Classical shell theory was applied with von Karman-Donnell type nonlinearity. Buckling load and post-buckling equilibrium paths have been calculated by singular perturbation technique. Esfahani et al. [27] studied buckling and post-buckling of FG Timoshenko beam under thermal loads with von Karman type non-linearity. The results revealed that buckling temperature, its shape and post-buckling equilibrium path greatly depends on temperature distribution. Noack et al. [28] developed new layer wise theory to account for layers with different thermal conductivities in addition to conduction, convection and radiation within those layers. Yiming Fu et al. [29] evaluated the buckling loads for Euler-Bernoulli beam which is subjected to one dimensional heat conduction. Galerkin's method has been adopted to obtain natural frequencies for FG beam with piezoelectric actuators. K. Dai et al. [30] have studied the active vibration control of FG beam using piezoelectric sensors and actuators under thermo-electro-mechanical conditions. They designed feedback control algorithm to control tip deflection and vibration of a beam in closed loop.

During the evolution of materials, it is found that addition of CNT which is good conductor of heat and shows superconductivity at low temperatures, improves thermal properties of FGM considerably. High Young's modulus and tensile strength gives enhanced mechanical properties. This has enabled the considerable scope for research in this field. Some important works in this direction are presented here. Shen and Zhang [31] carried out thermal buckling and post-buckling for Single Walled CNT reinforced FG plate. Micro-mechanical model has been used to obtain the material properties which were assumed to vary along thickness direction. It was found that reinforcement increases the buckling temperature and buckling strength. Shen [32] studied the nonlinear bending of plates made of FG nano composite reinforced with single walled CNT in simply supported conditions. Von Karman type nonlinearity was considered to find deflection and bending moment variation. It was found that there is significant effect of temperature variation, boundary conditions, slenderness ratio and CNT volume fraction on the bending of beam. The effect of CNT orientation was considered by Dong-Li Shi et al. [33]. They obtained the elastic properties of CNT reinforced composite for aligned and randomly oriented CNT by micromechanics

method to account for nanotube waviness and agglomeration and also the waviness and agglomeration significantly reduces the stiffness of material. Fidelus et al. [34] obtained thermo-mechanical properties of randomly oriented nano-composite practically. Nano-composite was examined for tensile Young's modulus and toughness for single walled and multi-walled nano tubes.

The objective of present work is to study free vibration analysis of carbon nanotube based functionally graded Timoshenko beam. Volume fraction of CNT is assumed to vary linearly along the thickness only. Applying first order shear deformation theory and constitutive relationship, strain and kinetic energy are calculated. Using finite element analysis Eigen values are evaluated for different boundary conditions. Mode shapes are plotted to visualise vibration response. This also includes the study of the free vibrations of functionally graded nano composite beams reinforced by randomly oriented straight single-walled carbon nanotubes within the framework of Timoshenko beam theory using finite element method. The material properties of the FG-CNTRC are assumed to be graded in the thickness direction and estimated though the Mori–Tanaka method because of its simplicity and accuracy even at a high volume fraction of inclusions. Finally, the effects of CNTs orientation, Effect of variation of volume fraction of CNT, slenderness ratios and boundary conditions on the dynamic characteristics of the beam are investigated. Using finite element analysis eigenvalues are evaluated for different boundary conditions. Mode shapes are also plotted for this case. Further the calculation of thermal stresses and strains for the FG-CNT Timoshenko beam is also considered as CNTs are having good thermal properties. First order shear deformation theory is assumed for displacement field. Strain-displacement and constituent relations are used to find out the final expressions for the stresses and strains. Nature of thermal behaviour has been observed for linear and exponential temperature distribution. Material properties are assumed to vary as per linear law for linear and power law of temperature distribution and as per exponential law for exponential of temperature distribution. Out of these conditions, first one is selected to find the effect of CNT orientation on thermal stresses and strains. Further FDM is applied to calculate the temperature distribution along the thickness of the beam. This temperature distribution is used to calculate stresses and strains in the beam. Comparing all these conditions conclusions are drawn for best distribution and effect of CNT orientation.

2.4 MOTIVATION AND OBJECTIVE OF THE WORK

Materials are invented based on the need for the application. Initially, metals and non-metals were invented, later polymers and ceramics. In this sequence, with the prime requirement of light weight and high strength, composites are invented. To improve the thermal stability at high temperature, FGMs are invented. During this evolution of materials, CNTs are introduced with excellent mechanical, thermal and electrical properties. Then a new concept is evolved to take advantages of both CNT and FGM is CNT based FGM. In current scenario, there is a lot of scope for research in this area. The study of material properties, mechanical properties, different types of analyses can be carried out on CNT based FGM to put it into the practical applications. Presently there are some areas where this material is being used, but by looking at the advantages of using this material, it should be used widely. With this motivation, present work is carried out.

The objectives of the present work are as stated below:

1. Finding out the material properties of CNT based FGM
2. Free Vibration Analysis of Timoshenko beam
3. Finding out the effect of CNT orientation
4. Thermal Analysis by analytical and finite difference method

Chapter 3

FREE VIBRATION ANALYSIS

Free vibration is the basic type of vibration in which the system vibrates with its natural frequency. The free vibration analysis carried out on CNT based FG Timoshenko beam is discussed in this chapter.

3.1 MODELLING OF BEAM

3.1.1 Calculation of Mechanical Properties of Beam

The modelling of beam starts with the calculation of material properties. As CNT volume is assumed to vary along the thickness only, material properties for each layer are calculated first and finally effective values for the entire beam are calculated. Here, linear variation of volume fraction of CNT (V_{cnt}) is considered. It is calculated by following formula,

$$V_{cnt} = (1-\frac{2z}{h})V_{cnt}^{*} \qquad (1)$$

Here, V_{cnt}^{*} depends on mass fraction and density of CNT and density of matrix and it is given by

$$V_{cnt}^{*} = \frac{\Lambda_{cnt}}{\Lambda_{cnt}} + (\rho^{cnt} / \rho^{m}) - (\rho^{cnt} / \rho^{m})\Lambda_{cnt}$$

where Λ_{cnt} called as is mass fraction of CNT. For uniform CNT distribution V_{cnt} equals to the V_{cnt}^{*}. After calculating volume fraction Young' modulus, Shear modulus, Poisson's ratio and Density of a beam can be calculated as follows,

$$\left.\begin{array}{ll} E = \eta_1 V_{cnt} E^{cnt} + V_m E^m & \dfrac{\eta_2}{G} = \dfrac{V_{cnt}}{G^{cnt}} + \dfrac{V_m}{G^m} \\ \upsilon = V_{cnt}\upsilon^{cnt} + V_m\upsilon_m & \rho = V_{cnt}\rho^{cnt} + V_m\rho_m \end{array}\right\} \qquad (2)$$

where, E^{cnt} & G^{cnt} are Young's modulus in longitudinal, transverse direction & shear modulus for carbon nano tube. E^m, G^m are Young's modulus & shear modulus for matrix (ceramic). η_j (j = 1, 2 and 3) is CNT efficiency parameter.

3.1.2 Problem Formulation

Here first order shear deformation theory is considered for Timoshenko beam. The axial and transverse displacements for this beam are as follows,

$$\left.\begin{aligned} u(x,y,z,t) &= u_0(x,t) - z\phi(x,t) \\ w(x,y,z,t) &= w_0(x,t) \end{aligned}\right\} \tag{3}$$

In this case three degrees of freedom per node has been considered. They are longitudinal displacement, transverse displacement (along Z axis) and angular rotation about Y axis. This is shown in *figure 3.1*.

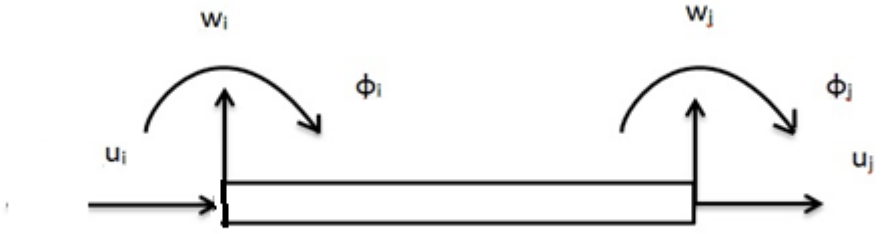

Figure 3.1 Degree of freedom for single element

Strain –displacement relation for small displacement can be derived from *equation (3)* as

$$\varepsilon_{xx} = \frac{\partial u_0}{\partial x} - z\frac{\partial \phi}{\partial x}, \qquad \gamma_{xz} = -\phi + \frac{\partial w_0}{\partial x}$$

From above equation, the constitutive relations can be formed for longitudinal and shear stress as

$$\begin{Bmatrix} \sigma_{xx} \\ \tau_{xz} \end{Bmatrix} = \begin{bmatrix} E(z) & 0 \\ 0 & G(z) \end{bmatrix} \begin{Bmatrix} \varepsilon_{xx} \\ \gamma_{xz} \end{Bmatrix}$$

Constitutive relations are formed to calculate strain energy and kinetic energy of beam. For given case the final expressions for these energies are as follows,

$$\left.\begin{aligned} U_b &= \frac{1}{2}\int_v (\sigma_{xx}\varepsilon_{xx} + \tau_{xz}\gamma_{xz})dAdx \\ T_b &= \frac{1}{2}\rho\int_v (\dot{u}^2 + \dot{w}^2)dAdx \end{aligned}\right\} \tag{4}$$

where, the symbol $(\dot{})$ shows the first differentiation of a property with respect to time. After this, Hamilton's principle is applied to get the differential equations in terms of two translational and one rotational degree of freedom i.e. u, w and ϕ. According to Hamilton's principle,

$$\int_{T_1}^{T_2} \left[\partial T_b - \partial U_b\right] dt = 0$$

Using *equation (4)* in above equation, the governing equations can be,

$$\delta u : I_0(x)\ddot{u}_0 - I_1(x)\ddot{\phi} - \frac{\partial}{\partial x}\left(A_{11}(x)\frac{\partial u_0}{\partial x} \right) + \frac{\partial}{\partial x}\left(B_{11}(x)\frac{\partial \phi}{\partial x} \right) = 0$$

$$\delta w : I_0(x)\ddot{w}_0 - \frac{\partial}{\partial x}\left(A_{55}(x)\left(\frac{\partial w}{\partial x} - \phi \right) \right) = 0 \qquad (5)$$

$$\delta \phi : I_2(x)\ddot{\phi} - I_1(x)\ddot{u}_0 + \frac{\partial}{\partial x}\left(B_{11}(x)\frac{\partial u_0}{\partial x} \right) - \frac{\partial}{\partial x}\left(D_{11}(x)\frac{\partial \phi}{\partial x} \right) - A_{55}(x)\left(\frac{\partial w}{\partial x} - \phi \right) = 0$$

The values of stiffness coefficients and mass moments from *equation (5)* are given below. K_s is shear correction factor.

$$\left[A_{11}(x) \quad B_{11}(x) \quad D_{11}(x) \right] = \int_A E(z)\left[1 \quad z \quad z^2 \right] dA$$

$$A_{55}(x) = \int_A K_s G(z) dA$$

$$\left[I_0(x) \quad I_1(x) \quad I_2(x) \right] = \int_A \rho(z)\left[1 \quad z \quad z^2 \right] dA$$

3.1.3 Finite Element Analysis

To solve the above governing equation Finite element analysis is implemented. Finite element analysis aim is to find out the field variables (displacement) at nodal points by approximate analysis. These field variables are related to the field variables of nodal points inside the element. Here employing the approximate solution method the governing equations are approximated by a system of ordinary differential equations.

The solution of the above partial differential equations is assumed in the following form

$$\begin{aligned} u_0 &= c_1 + c_2 x + c_3 x^2, \\ w_0 &= c_4 + c_5 x + c_6 x^2 + c_7 x^3, \\ \phi &= c_8 + c_9 x + c_{10} x^2 \end{aligned} \qquad (6)$$

In above equation, the order of interpolation of slope is less than that of order of transverse displacement. This is to avoid the shear locking of the element. Some constants from above equation can be defined as

$$c_3 = \frac{\mu(c_8 - c_5)}{2}, \quad c_7 = \frac{\eta(c_8 - c_5)}{6}, \quad c_6 = \frac{c_9}{2}, \quad c_{10} = \frac{\eta(c_8 - c_5)}{2}$$

where,

$$\mu = \frac{B_{11}A_{55}}{(A_{11}D_{11} - B_{11}^2)}, \qquad \eta = \frac{A_{11}A_{55}}{(A_{11}D_{11} - B_{11}^2)}, \qquad \delta = \frac{1}{12 + \eta l_e^2}$$

So, the longitudinal, transverse displacement and angular rotation in terms of field variables can be written as,

$$\{u\} = [N(x)]\{a\}$$

In above equation $[N(x)]$ is matrix having functions of x and $\{a\}$ is vector of independent constants. Applying the boundary conditions at node 1 and 2 respectively depending upon the end supports, shape functions for each case can be obtained.

$$[G]^{-1} = \begin{bmatrix} N(1) \\ N(2) \end{bmatrix} \qquad \{a\} = [G]\{\hat{u}\}$$

Here, $\{\hat{u}\}$ is the nodal displacement vector. So, further

$$\{u\} = [N(x)]\{a\} = [N(x)][G]\{\hat{u}\} = [\psi(x)]\{\hat{u}\}$$

The $\psi(x)$ represents matrix of exact shape functions. For this case, $\psi^u(x), \psi^w(x)$ and $\psi^\phi(x)$ gives the exact shape functions for axial displacement, transverse displacement and angular rotation respectively. The values of these shape functions are given below,

$$\psi_{11}^u = (1 - x/l_e), \quad \psi_{12}^u = 6\mu\delta(x/l_e - 1), \quad \psi_{13}^u = 3\mu\delta x(x - l_e),$$

$$\psi_{14}^u = x/l_e, \qquad \psi_{15}^u = -\psi_{12}^u, \qquad \psi_{16}^u = \psi_{13}^u$$

$$\psi_{11}^w = 0, \quad \psi_{12}^w = \frac{\delta}{l_e}(\eta l_e{}^3 + 12l_e - 12x + 2\eta x^3 - 3\eta x^2 l_e),$$

$$\psi_{13}^w = \frac{x\delta}{l_e}(\eta l_e{}^3 + 6l_e - 6x + \eta x^2 l_e - 2\eta x^2 l_e), \quad \psi_{14}^w = 0,$$

$$\psi_{15}^w = \frac{x\delta}{l_e}(-12 + 2\eta x^2 - 2\eta x l_e{}^2), \quad \psi_{16}^w = \frac{x\delta}{l_e}(-6l_e + 6x + \eta x^2 l_e - \eta x l_e{}^2)$$

$$\psi_{11}^\phi = 0, \quad \psi_{12}^\phi = \frac{6x\delta\eta}{l_e}(-l_e + x), \quad \psi_{13}^\phi = \frac{\delta}{l_e}(\eta l_e{}^3 + 12l_e - 12x + 3\eta x^2 l_e - 4\eta x^2 l_e),$$

$$\psi_{14}^\phi = 0, \quad \psi_{15}^\phi = -\psi_{12}^\phi, \quad \psi_{16}^\phi = \frac{x\delta}{l_e}(12 + 3\eta x l_e - 2\eta l_e{}^2)$$

Finally, the equation of motion is derived as follows,

$$[M]\{\ddot{q}\} + [K]\{q\} = \{F\}$$

where, $[M]$ denotes the global mass matrix and $[K]$ denotes the global stiffness matrix. Initially, elemental stiffness and mass matrices need to find out. The elemental stiffness matrix can be obtained as given,

$$\left[K^e\right] = \int_0^{l_e} [B]^T [D][B]\, dx$$

In this equation $[B]$ is strain displacement matrix and $[D]$ is constitutive matrix. Integrating above equation the elemental stiffness matrix can be obtained. The stiffness matrix is symmetric, so the terms in upper triangular matrix are given below and remaining terms are zero.

$$K_{11}^e = -K_{14}^e = \frac{A_{11}^e}{l_e}, \quad K_{13}^e = -K_{16}^e = -\frac{B_{11}^e}{l_e},$$

$$K_{22}^e = -K_{25}^e = \frac{A_{55}^e \psi^e}{l_e}, \quad K_{23}^e = K_{26}^e = \frac{A_{55}^e \psi^e}{2},$$

$$K_{33}^e = K_{66}^e = \frac{D_{11}^e}{l_e} + \frac{A_{55}^e \psi^e l_e}{4}, \quad K_{34}^e = -K_{13}^e, \quad K_{35}^e = -K_{25}^e,$$

$$K_{36}^e = -\frac{D_{11}^e}{l_e} + \frac{A_{55}^e \psi^e l_e}{4},$$

$$K_{44}^e = -K_{11}^e, \quad K_{46}^e = -K_{13}^e, \quad K_{55}^e = -K_{22}^e, \quad K_{56}^e = -K_{23}^e$$

Similarly, elemental stiffness matrix can be obtained by using following formula.

$$\left[M^e\right] = \int_0^{l_e} [\rho][N]^T [N]\, dx$$

Following elements of mass matrix can be obtained by solving above equation.

$$M_{11}^e = 2M_{14}^e = M_{44}^e = \frac{1}{3} I_0^e l_e^2, \quad M_{12}^e = -M_{45}^e = -\frac{1}{2} I_0^e l_e^2 \mu^e \psi^e + \frac{1}{2} I_1^e l_e^2 \eta^e \psi^e,$$

$$M_{13}^e = -\frac{1}{12} \psi^e l_e \left(3 I_0^e l_e^2 \mu_e + I_1^e \eta_e l_e^2 + 48 I_1^e\right),$$

$$M_{15}^e = \frac{1}{2} I_0^e l_e^2 \mu^e \psi^e - \frac{1}{2} I_1^e l_e^2 \eta^e \psi^e, \quad M_{16}^e = \frac{1}{12} \psi^e l_e \left(3 I_0^e l_e^2 \mu_e + I_1^e \eta_e l_e^2 - 24 I_1^e\right),$$

$$M_{22}^e = \frac{1}{35} (\psi^e)^2 l_e (42 I_o^e (\mu^e)^2 l_e^2 + 13 I_0^e (\eta^e)^2 l_e^4 + 294 I_0^e \eta_e l_e^2 + 1680 I_0^e + 42 I_2^e (\eta_e)^2 {l_e}^2 - 84 I_1^e \mu^e \eta^e l_e^2),$$

$$M_{23}^e = -M_{56}^e = \frac{1}{210} (\psi^e)^2 l_e^2 (126 I_o^e (\mu^e)^2 l_e^2 + 231 I_0^e \eta^e l_e^2 - 147 I_1^e \mu^e \eta_e l_e^2 + 11 I_0^e (\eta_e)^2 {l_e}^4 + 21 I_2^e (\eta_e)^2 {l_e}^2 + 1260 I_2^e \eta^e),$$

$$M_{24}^e = -\frac{1}{2} I_0^e l_e^2 \mu^e \psi^e + \frac{1}{2} I_1^e l_e^2 \eta^e \psi^e,$$

$$M_{25}^e = -\frac{3}{70}(\psi^e)^2 l_e(28I_o^e(\mu^e)^2 l_e^2 - 3I_0^e(\eta^e)^2 l_e^4 - 84I_0^e\eta_e l_e^2 - 560I_0^e + 28I_2^e(\eta_e)^2 l_e{}^2 - 56I_1^e\mu^e\eta^e l_e^2),$$

$$M_{26}^e = -M_{35}^e = \frac{1}{420}(\psi^e)^2 l_e^2(252I_o^e(\mu^e)^2 l_e^2 - 13I_0^e(\eta^e)^2 l_e^2 - 378I_0^e\eta_e l_e^2 - 2520I_0^e + 42I_2^e(\eta_e)^2 l_e{}^2 - 2520I_2^e\eta^e - 294I_1^e\mu^e\eta^e l_e^2 + 2520I_1^e\mu^e),$$

$$M_{33}^e = \frac{1}{210}(\psi^e)^2 l_e(63I_o^e(\mu^e)^2 l_e^4 - 2I_0^e(\eta^e)^2 l_e^6 - 21I_1^e\mu^e\eta_e l_e^4 + 28I_2^e(\eta_e)^2 l_e{}^4 + 42I_2^e(\eta_e)^2 l_e{}^4 + 420I_2^e(\eta_e)^2 l_e{}^2 + 1260I_1^e\mu^e l_e^2 + 252I_0^e l_e^2 + 10080I_2^e),$$

$$M_{34}^e = -\frac{1}{4}I_0^e l_e^3\mu^e\psi^e + \frac{1}{12}I_1^e l_e^3\eta^e\psi^e - 2I_1^e l_e\psi^e,$$

$$M_{36}^e = -\frac{1}{420}(\psi^e)^2 l_e(-126I_o^e(\mu^e)^2 l_e^4 + 3I_0^e(\eta^e)^2 l_e^6 + 84I_0^e\eta_e l_e^4 + 504I_0^e l_e{}^2 + 14I_2^e(\eta_e)^2 l_e{}^4 + 840I_2^e\eta_e l_e{}^2 + 10080I_2^e + 42I_1^e\mu^e l_e^4\eta_e - 2520I_1^e\mu^e l_e^2),$$

$$M_{46}^e = -\frac{1}{4}I_0^e l_e^3\mu^e\psi^e - \frac{1}{12}I_1^e l_e^3\eta^e\psi^e - 4I_1^e l_e\psi^e,$$

$$M_{55}^e = \frac{6}{5}I_o^e(\mu^e)^2(\psi^e)^2 l_e^3 + \frac{13}{35}I_o^e(\psi^e)^2(\eta^e)^2 l_e^5 + \frac{42}{5}I_o^e(\psi^e)^2\eta^e l_e^3 + 48I_o^e(\psi^e)^2 l_e + \frac{6}{5}I_2^e(\eta^e)^2(\psi^e)^2 l_e^3 - \frac{12}{5}I_1^e\mu^e(\psi^e)^2 l_e^3\eta^e,$$

$$M_{56}^e = \frac{3}{10}I_o^e(\mu^e)^2(\psi^e)^2 l_e^5 + \frac{1}{105}I_o^e(\psi^e)^2(\eta^e)^2 l_e^7 + \frac{6}{5}I_o^e(\psi^e)^2 l_e^3 + \frac{2}{15}I_2^e(\psi^e)^2(\eta^e)^2 l_e^5 + 2I_2^e\eta^e(\psi^e)^2 l_e^3 + 48I_2^e(\psi^e)^2 l_e - \frac{1}{10}I_1^e\mu^e(\psi^e)^2 l_e^5\eta^e + 6I_1^e\mu^e(\psi^e)^2 l_e^3,$$

3.2 VALIDATION OF PRESENT THEORY

Based upon the present theory a Matlab code has been developed and implemented to a beam with h = 0.1 m, L/h = 10 to study the convergence of non-dimensional fundamental frequency for V_{cnt}^* = 0.12. It is calculated by following formula,

$$\Omega = \frac{\omega L^2}{h}\sqrt{\frac{\rho_m}{E_m}}$$

The material properties of the beam are as given in *table 3.1*.

Table 3.1 Material Properties of Beam

Material Property	CNT	Matrix
Young' Modulus (GPa)	600	2.5
Poisson's Ratio	0.19	0.3
Density (Kg/m^3)	1130	1190

Table 3.2 shows the non-dimensional frequency for different no. of elements.

Table 3.2 Variation of non-dimensional frequency for different no. of elements

No of Elements	Non-dimensional Frequency (Ω)
2	1.8193
5	1.6748
10	1.6540
15	1.6501
20	1.6488
21	1.6486

The graph is plotted between no. of elements along X-axis and non-dimensional frequency along Y- axis.

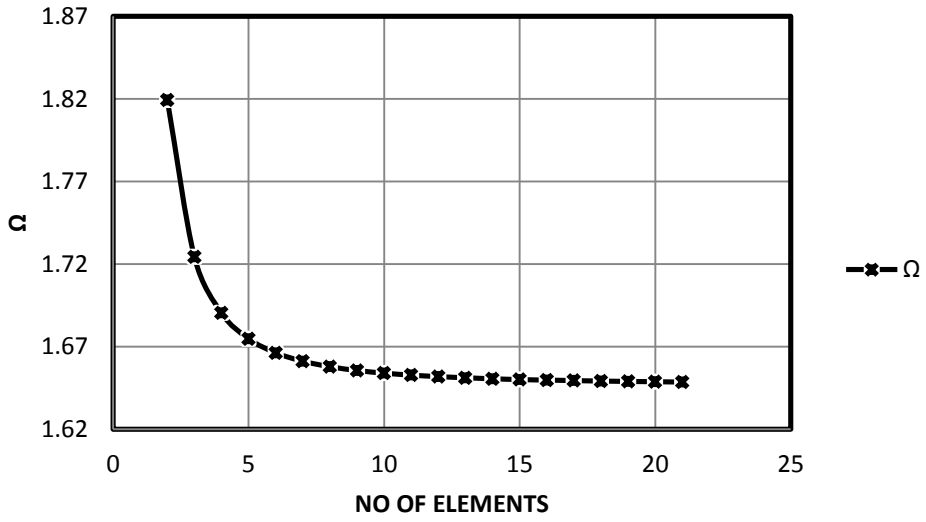

Figure 3.2 Convergence study

From the *table 3.2* and *figure 3.2* it is found that, the result converges for 21 no. of elements. So, for further analysis 21 elements were used

Now, present theory is validated for V_{cnt}^{*} = 0.12, 0.17 and 0.28. Results are obtained with both ends of the beam clamped and it is compared with the results given by Liao-Liang KE at al [9]. *Table 3.3* compares present non-dimensional fundamental frequencies with the results available in literature. From the table it is found that the results agree well with reference.

Table 3.3 Comparison of non-dimensional fundamental frequencies

S. No.	V_{cnt}^{*}	Ω_{ref}	$\Omega_{present}$
1	0.12	1.6063	1.6490
2	0.17	2.0557	2.0898
3	0.28	2.33250	2.2256

Proposed theory is also validated by comparing static deflection of free end of cantilever beam with that presented by Hossein Rokni et al. [36]. The beam dimensions are *L = 0.14 m, b = 0.02 m and h = 0.01 m.* For this case the assumed material properties are given in *table 3.4* below.

Table 3.4 Material properties of beam

Material Property	CNT	Matrix
Young' Modulus (GPa)	900	1.9
Poisson's Ratio	0.28	0.34
Density (Kg/m^3)	2100	1050

The deflection at the free end of the beam is calculated by following formula,

$$\delta = \frac{FL^3}{3EI}$$

Here, force of magnitude *19.6 N* is applied at the free end, *I* is the moment of inertia of the beam, *E* is effective Young's modulus of the beam. *Table 3.5* shows comparison between results obtained for reference and present case.

Table 3.5 Comparison of results for cantilever beam

S. No.	Property	Reference	Present
1	Effective Young's Modulus *E* (Gpa)	3.5979	3.4347
2	Deflection At Free End (mm)	2.9897	3.1316

3.3 PRESENT RESULTS

Now, the results are obtained for above beam with simply supported end conditions for varying volume fraction of CNT. The effect of variation of volume fraction of CNT on non-dimensional fundamental frequency is shown in *table 3.6* for slenderness ratio equal to *10* in all cases.

Table 3.6 Effect of variation of volume fraction of CNT on non-dimensional fundamental frequency

S. No.	CNT Volume Fraction (V_{cnt})	Non-dimensional Frequency (Ω)
1	0.1	0.8118
2	0.2	0.9293
3	0.3	1.0307

From above table it is found that non-dimensional frequency increases as volume fraction of CNT increases. Now, the results are obtained to observe the effect of slenderness ratio on dimensional frequency for constant CNT volume fraction. *Table 3.7* shows effect of slenderness ratio (L/h) on non-dimensional fundamental frequency with V_{cnt} *=0.1*. It shows that as *L/h* ratio increases frequency also increases.

Table 3.7 Effect of slenderness ratio on non-dimensional fundamental frequency

S. NO.	*L/h* Ratio	Non-dimensional Frequency (Ω)
1	10	0.5805
2	20	1.1632
3	30	1.7506
4	40	2.3450
5	50	2.9490

Finally, mode shapes are plotted for first case of *table 3.7*. First five modes are shown in *figure 3.3*. Mode shapes are the vibration patterns for the particular frequency and they are obtained from Eigen vectors.

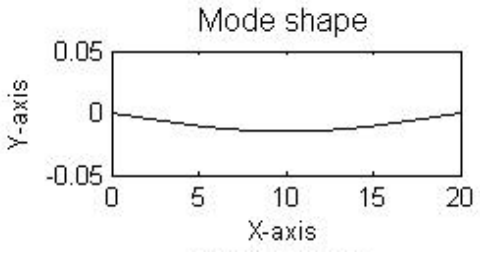

First mode shape

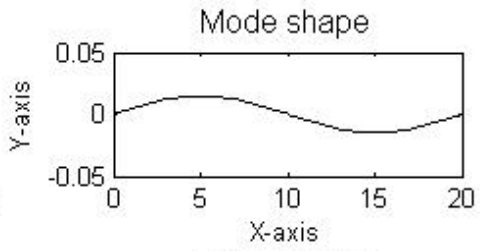

Second mode shape

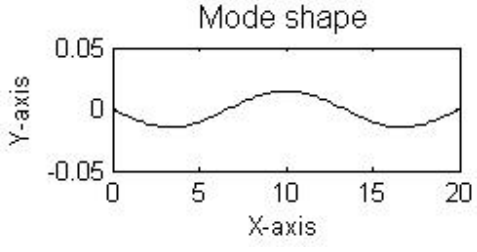

Third mode shape

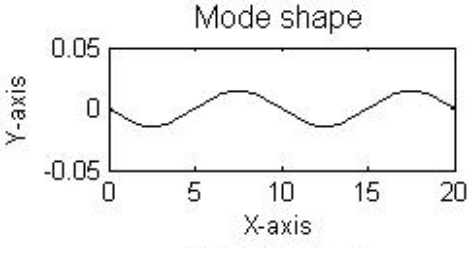

Fourth mode shape

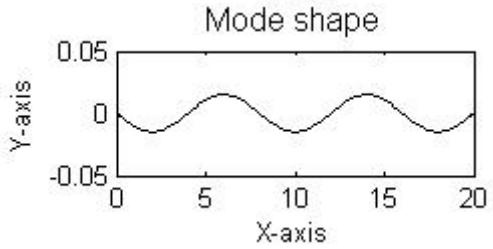

Fifth mode shape

Figure 3.3 Five mode shapes corresponding to first five natural frequencies

Now, the dynamic analysis is carried out for given beam. Displacement versus time diagram is plotted to understand the time response with varying CNT volume fraction. For simply supported case, the maximum displacement obtained for v_{cnt} =0.1, 0.2 and 0.3 are 0.029 m, 0.022 m and 0.016 m respectively. *Figure 3.4* shows the response of sinusoidal force of magnitude $100\sin(80t)$ for same case of mode shapes for 0.45 seconds.

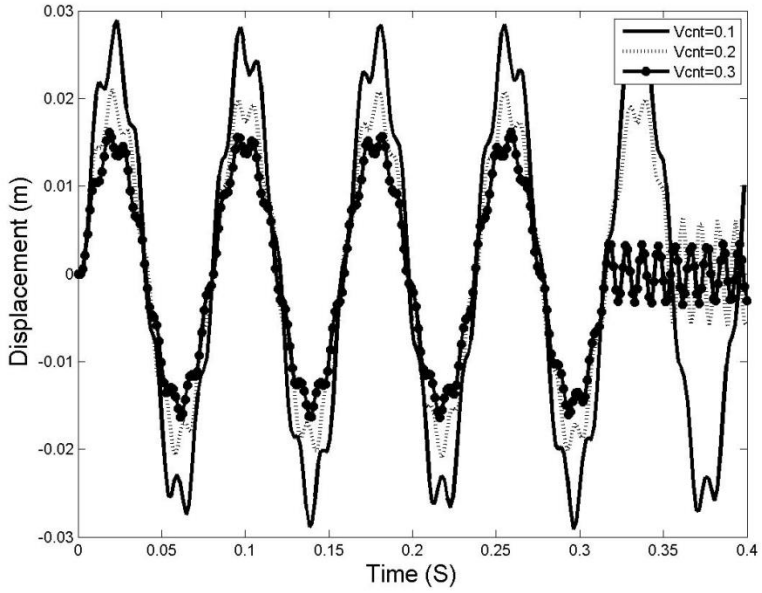

Figure 3.4 Displacement vs. Time graph for v_{cnt}^{*} =0.1, 0.2, 0.3

Chapter 4

EFFECT OF CARBON NANO TUBE ORIENTATION

In the previous analysis the CNTs are assumed to be unidirectional along the length. But practically, it is not possible. The effect of CNT orientation on natural frequency is discussed in this chapter.

4.1 MATERIAL PROPERTIES OF FG-CNTRC

An embedded carbon nanotube in a polymer matrix is considered to be replaced with an equivalent long fibre for predicting the mechanical properties of the carbon nanotube/polymer composite. The inverse rule of mixture is used for calculating material properties of equivalent fibre [7]

$$E_{LEF} = \frac{E_{LC}}{V_{EF}} - \frac{E_m V_m}{V_{EF}}$$
$$\frac{1}{G_{EF}} = \frac{1}{G_C V_{EF}} - \frac{V_m}{G_m V_{EF}} \qquad (7)$$
$$\upsilon_{EF} = \frac{\upsilon_C}{V_{EF}} - \frac{\upsilon_m V_m}{V_{EF}}$$

where, *E*, *G*, υ and *V* are the longitudinal Young's modulus, Shear modulus, Poisson's ratio and Volume fraction respectively. Suffixes *EF*, *C* and *m* show properties for equivalent fibre, CNT and matrix material respectively. The equivalent fibre for SWCNT with chiral index of (10, 10) is a solid cylinder with diameter of 1.424 nm. Material properties for this CNT taken from reference are mentioned in *Table 4.1*.

Table 4.1 Material properties of equivalent fibre

Mechanical property	Equivalent fibre**[9]**
Longitudinal Young's modulus (E_{LEF})	649.12 (GPa)
Transverse Young's modulus (E_{TEF})	11.27 (GPa)
Longitudinal shear modulus (G_{EF})	5.13 (GPa)
Poisson's ratio (υ_{EF})	0.284

4.2 MODELLING OF BEAM

The effect of randomly oriented, straight CNTs is formulated here. The orientation of a straight CNT is characterized by two Euler angles α and β, as shown in *Figure 4.1*. Thus

giving rise to the base vectors $\vec{e}_i$ of the global (0 -$x_1x_2x_3$) and $\vec{e}_i^{'}$ of the local coordinate systems (0- $x^{'}_1x^{'}_2x^{'}_3$) which are related through the transformation matrix g:

$$\vec{e}_i = g\vec{e}_i^{'}$$

Where g is given by:

$$g = \begin{bmatrix} \cos\beta & -\cos\alpha\sin\beta & \sin\alpha\sin\beta \\ \sin\beta & \cos\alpha\cos\beta & -\sin\alpha\cos\beta \\ 0 & \sin\alpha & \cos\alpha \end{bmatrix}$$

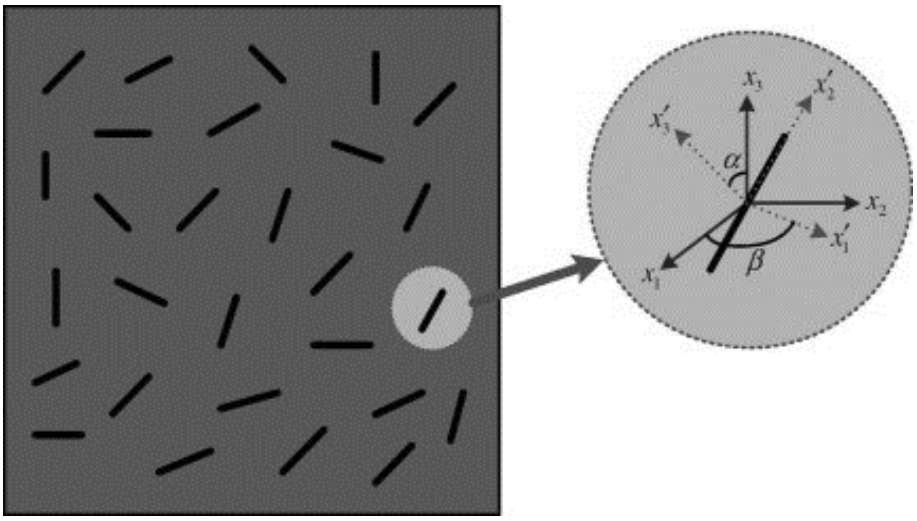

Figure 4.1 Representative volume element (RVE) with randomly oriented, straight CNTs. [7]

The orientation distribution of CNTs in a composite is characterized by a probability density function $p(\alpha,\beta)$ satisfying the normalizing condition.

$$\int_0^{2\pi}\int_0^{\pi/2} p(\alpha,\beta)\sin\alpha d\alpha d\beta = 1$$

Consider CNTs to be completely randomly oriented, the density function for this case is:

$$p(\alpha,\beta) = \frac{1}{2\pi}$$

The Hill's elastic moduli of the reinforcing phase can be calculated from the equality of following two matrices [7]:

$$C_r = \begin{bmatrix} n_r & l_r & l_r & 0 & 0 & 0 \\ l_r & k_r + m_r & k_r - m_r & 0 & 0 & 0 \\ l_r & k_r - m_r & k_r + m_r & 0 & 0 & 0 \\ 0 & 0 & 0 & p_r & 0 & 0 \\ 0 & 0 & 0 & 0 & m_r & 0 \\ 0 & 0 & 0 & 0 & 0 & p_r \end{bmatrix}$$

$$C_r = \begin{bmatrix} 1/E_{LEF} & -\upsilon_{EF}/E_{LEF} & -\upsilon_{EF}/E_{LEF} & 0 & 0 & 0 \\ -\upsilon_{EF}/E_{LEF} & 1/E_{LEF} & -\upsilon_{EF}/E_{LEF} & 0 & 0 & 0 \\ -\upsilon_{EF}/E_{LEF} & -\upsilon_{EF}/E_{LEF} & 1/E_{LEF} & 0 & 0 & 0 \\ 0 & 0 & 0 & 1/G_{EF} & 0 & 0 \\ 0 & 0 & 0 & 0 & 1/G_{EF} & 0 \\ 0 & 0 & 0 & 0 & 0 & 1/G_{EF} \end{bmatrix}^{-1}$$

where, C_r is the stiffness tensor of the equivalent fibres and when CNTs are assumed randomly oriented in the matrix, the composite is assumed to be isotropic then bulk modulus K and shear modulus G of the beam are derived as,

$$K = K_m + \frac{V_{cnt}(\delta_r - 3K_m\alpha_r)}{3(V_m + V_{cnt}\alpha_r)}$$
$$G = G_m + \frac{V_{cnt}(\eta_r - 2G_m\beta_r)}{2(V_m + V_{cnt}\beta_r)} \quad (8)$$

Finally, Young's modulus for oriented CNT considering modified shear and bulk modulus will be,

$$E = \frac{9KG}{3K + G} \quad (9)$$

Keeping all other values constant and using Young's modulus from above equation, *equations (4), (5)* and *(6)* are modified to obtain the effect of CNT orientation on elemental stiffness and mass matrices.

As CNT volume is assumed to vary along the thickness only, material properties for each layer are calculated first and finally effective values for entire beam are calculated. Here, linear variation of volume fraction of symmetrical CNT (V_{cnt}) is considered. It is calculated by following formula:

$$V_{cnt} = \frac{4|z|}{h} V_{cnt}^*$$

4.3 RESULTS AND DISSCUSSION

This theory has been implemented to a beam with h = 1 m, L/h = 20 to study the convergence of non-dimensional fundamental frequency for V_{cnt}^{*} = 0.075. It is calculated by following formula:

$$\lambda^2 = \omega L^2 \sqrt{\frac{\rho_m A}{E_m I}}$$

Now, with the material properties assumed for the beam are as mentioned in the *table 4.2*.

Table 4.2 Material properties of beam

Material Property	CNT	Matrix
Young' Modulus (GPa)	900	10
Poisson's Ratio	0.28	0.3
Density (Kg/m^3)	2100	1150

With these properties and applying the present theory, results of the first five non-dimensional frequencies for clamped–clamped (C–C) are obtained. The effect on SFG-CNTR beam based on Timoshenko beam theory with different number of elements is obtained to study the convergence and is shown in *table 4.3*. Graph is also plotted to observe the convergence as shown in *figure 4.2*. It is observed from *figure 4.2* and *table 4.3* that the convergence of the present results occur with a number of element N = 100.

Table 4.3 Effect of number of elements on non-dimensional fundamental frequency

Mode No.	20	40	60	80	100
1	5.7046	5.4562	5.4229	5.4089	5.4030
2	7.7632	7.7280	7.6686	7.6506	7.6413
3	9.6638	9.4572	9.3968	9.3708	9.3599
4	9.8956	10.9441	10.8519	10.8237	10.8090
5	11.7088	12.2242	12.1418	12.1037	12.0874

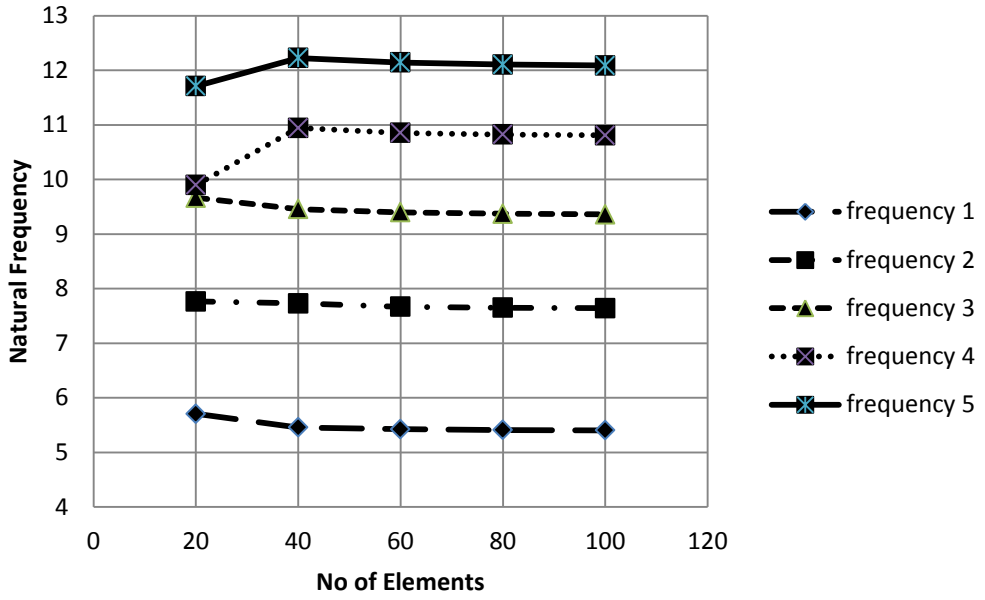

Figure 4.2 Convergence study with consideration of CNT orientation

To validate the results beam slenderness ratio L/h = 20 and V_{cnt}^{*} = 0.075 are selected with clamped–clamped condition of Timoshenko beam and are verified with the results given by Yas and Heshmati [7].

Table 4.4 compares the effect of variation of volume fraction of CNT on dimensionless fundamental frequency. The first five frequencies for Clamped–Clamped, SFG-CNTRC beams are shown in the table:

Table 4.4 Effect of variation of volume fraction of CNT on non-dimensional fundamental frequency

Mode No.	CNT Volume Fraction (V_{cnt})				
	0.075	0.1	0.125	0.15	0.175
1	5.4030	5.7963	6.1273	6.4122	6.6630
2	7.6413	8.1981	8.6656	9.0706	9.4244
3	9.3599	10.0411	10.6146	11.1080	11.5424
4	10.8090	11.5967	12.2579	12.8307	13.3311
5	12.0874	12.9672	13.7077	14.3448	14.9053

From this table it is clear that the values of natural frequencies increase due to the effect of CNT orientation.

Table 4.5 shows effect of slenderness ratio (*L/h*) on non-dimensional fundamental frequency. Frequencies are calculated for slenderness ratios 20, 40, 60 and 80. It is found that as *L/h* ratio increases frequency also increases.

Table 4.5 Effect of slenderness ratio on non-dimensional fundamental frequency

Mode No.	*L/h* = 20	*L/h* = 40	*L/h* = 60	*L/h* = 80
1	5.4030	7.6883	9.5166	11.1623
2	7.6413	10.8722	13.4554	15.7780
3	9.3599	13.3185	16.4855	19.3357
4	10.8090	15.3790	19.0325	22.3165
5	12.0874	17.1994	21.2886	24.9678

Displacement versus time diagram is plotted to understand the time response with varying CNT volume fraction. *Figure 4.3* shows the response of sinusoidal force of magnitude *100 N* which is acting at the centre of the beam with clamped-clamped boundary condition of FG beam and exciting frequency of *80 Hz*. The maximum displacement in this case is found to be 0.09 micrometres.

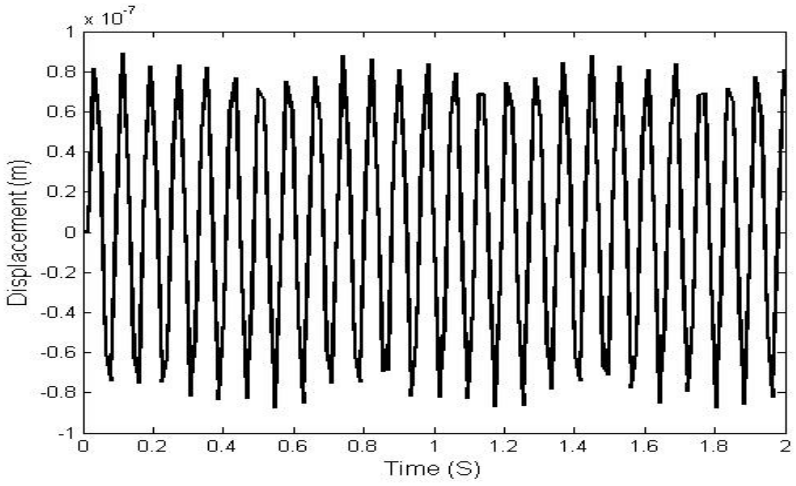

Figure 4.3 Plot of Displacement Vs. time of CNT based FG beam under sinusoidal loading

Chapter 5

THERMAL ANALYSIS

Thermal analysis for the CNT based FG Timoshenko beam is carried out by two methods. First is by considering analytical method for finding out the temperature distribution and second is FDM for finding out the temperature distribution. The modelling of the beam, effect of temperature distribution on strains and stresses by both these methods and effect of CNT orientation in each case is discussed in this chapter.

A] ANALYTICAL METHOD FOR TEMPERATURE DISTRIBUTION

5.1 (CASE I) EXPONENTIAL MATERIAL DISTRIBUTION WITH EXPONENTIAL TEMPERATURE DISTRIBUTION

5.1.1 Temperature Distribution

For this case exponential temperature distribution is assumed. The expression for temperature distribution along the thickness direction for one dimensional heat conduction is as below,

$$T_e(z) = A_e + B_e e^{\beta h} \tag{10}$$

With thermal boundary conditions $T_{(-h/2)} = T_m$ and $T_{(h/2)} = T_{cnt}$, the values of constants A_e and B_e can be as below,

$$A_e = \frac{T_m e^{\beta h} - T_{cnt}}{e^{\beta h} - 1}, \qquad B_e = \left(T_{cnt} - \frac{T_m e^{\beta h} - T_{cnt}}{e^{\beta h} - 1} \right) e^{-\beta h}$$

Using the above values of constants in *eq. (10),* the final expression for temperature distribution is as below,

$$T_e(z) = \frac{T_m e^{\beta h} - T_{cnt}}{e^{\beta h} - 1} + \left(T_{cnt} - \frac{T_m e^{\beta h} - T_{cnt}}{e^{\beta h} - 1} \right) e^{\beta (z-h)} - T_0 \tag{11}$$

5.1.2 Material Properties

FG beam is assumed to be made of graded SWCNTs along the thickness direction according to exponential law. The volume fraction distribution of the CNT, according to this law, can be,

$$V_{cnt} = 1 - e^{\left(z/h + 0.5\right)} \tag{12}$$

where, *h* is the thickness and *z* is co-ordinate along the thickness. So, the material properties required are Young's modulus, thermal conductivity and co-efficient of thermal expansion which are varied as per following rule (*equation 13*) respectively,

$$\begin{aligned} E(z) &= E_{cm}\left(1-e^{(z/h+0.5)}\right)+E_m, \\ k(z) &= k_{cm}\left(1-e^{(z/h+0.5)}\right)+k_m, \\ \alpha(z) &= \alpha_{cm}\left(1-e^{(z/h+0.5)}\right)+\alpha_m \end{aligned} \tag{13}$$

Here the constants are as defined below,

$$E_{cm}=(E_{cnt}-E_m), \qquad k_{cm}=(k_{cnt}-k_m), \qquad \alpha_{cm}=(\alpha_{cnt}-\alpha_m)$$

Suffixes 'cnt' and 'm' represent properties of CNT and matrix material respectively.

5.1.3 Determination of Stress and Strain

According to FSDT and the axial displacement of the beam from neutral axis is,

$$u(x,z)=u_0-z\frac{\partial w}{\partial x}+z\beta_y \tag{14}$$

In above expression u_0 represents middle surface displacement, *w* is deformation along transverse direction and β_y is rotation of the vertical line. Now, using strain-displacement relation, the expression for strain can be obtained as,

$$\varepsilon_{xx}=\frac{\partial u(x,z)}{\partial x}=\frac{\partial u_0}{\partial x}-z\frac{\partial^2 w}{\partial x^2}+z\frac{\partial \beta_y}{\partial x} \tag{15}$$

Above equation gives strain along the x-direction. Now, using constitutive relations with plain strain condition, the expression for thermal stresses developed in the beam along x-direction can be,

$$\sigma_{xx}(z)=\frac{E(z)}{1-\nu}\left[\frac{\varepsilon_{xx}}{1+\nu}-\alpha(z)T_e(z)\right] \quad =\frac{E(z)}{1-\nu^2}\left[\frac{\partial u_0}{\partial x}-z\frac{\partial^2 w}{\partial x^2}+z\frac{\partial \beta_y}{\partial x}-\alpha(z)T_e(z)(1+\nu)\right] \tag{16}$$

In above equation there are three unknowns $\frac{\partial u_0}{\partial x}$, $\frac{\partial^2 w}{\partial x^2}$ and $\frac{\partial \beta_y}{\partial x}$. To evaluate these constants, three boundary conditions with equilibrium equations are applied.

First boundary condition will be resultant force in X direction is zero in equilibrium. i.e.

$$\sum F_x=0 \Rightarrow \int_{-h/2}^{h/2}\sigma_{xx}(z)bdz=0$$

Second boundary condition will be resultant moment about Y axis, considering just thermal effect,

$$\frac{\partial^2 w}{\partial x^2} I_y \int_{-h/2}^{h/2} E(z)dz = -M_{Ty}$$

where, M_{Ty} is the resultant thermal moment about Y axis and I_y is moment of inertia which can be defined as,

$$M_{Ty} = b\int_{-h/2}^{h/2} zE(z)\alpha(z)T(z)dz, \qquad I_y = \frac{bd^3}{12}$$

Third boundary condition will be total moment acting on the beam for simply supported case will zero at two end points.

$$\int_{-h/2}^{h/2} \sigma_{xx}(z)zbdz = 0; \qquad x = 0, x = l$$

Let,

$$C_1 = \frac{\partial u_0}{\partial x}, \qquad C_2 = \frac{\partial^2 w}{\partial x^2}, \qquad C_3 = \frac{\partial \beta_y}{\partial x} \tag{17}$$

Applying above boundary conditions with following conventional definitions,

$$I_0 = \int_{-h/2}^{h/2} e^{\lambda z}dz, \qquad I_{0T} = \int_{-h/2}^{h/2} \alpha_0 e^{(\lambda+\omega)z}T(z)dz,$$
$$I_1 = \int_{-h/2}^{h/2} ze^{\lambda z}dz, \qquad I_{1T} = \int_{-h/2}^{h/2} z\alpha_0 e^{(\lambda+\omega)z}T(z)dz,$$
$$I_2 = \int_{-h/2}^{h/2} z^2 e^{\lambda z}dz, \quad I_{2T} = \int_{-h/2}^{h/2} z\alpha_0 e^{\omega z}T(z)dz$$

The new set of equations for the system can be obtained as given below,

$$I_0C_1 - (C_2 - C_3)I_1 = I_{0T}$$
$$I_0C_1 - (C_2 - C_3)I_0 = I_{1T}$$
$$C_2 = (-I_{1T} \times b) / (I_y \times I_0)$$

Solving above equations the constants C_1, C_2 and C_3 can be obtained. The expressions for these constants are given below,

$$C_1 = \frac{I_{1T}I_1 - I_{0T}I_2}{I_0I_2 - I_{12}}, \qquad C_2 = \frac{-I_{1t}b}{I_yI_0}$$
$$C_3 = \frac{I_1I_{0T}I_yI_0 + bI_0I_{1T}I_2 - I_0^2I_yI_{1T} - bI_1^2I_{1T}}{I_yI_0(I_0I_2 - I_1^2)}$$

So, these values are placed in *equation (15)* and *(16)* and the final expression for strain and stress can be obtained as below,

$$\varepsilon = \frac{1}{1-\nu^2}\left(C_1 - zC_2 + zC_3 + \alpha(z)T_e(z)(1+\nu)\right)$$
$$\sigma = E(z)\varepsilon \tag{18}$$

From *equation (18),* it is found that stresses and strains are the functions of temperature distribution and temperature distribution is a function of distance of a layer from middle surface and thermal boundary conditions.

5.2 (CASE II) LINEAR TEMPERATURE DISTRIBUTION WITH LINEAR AND POWER LAW MATERIAL PROPERTY VARIATION

5.2.1 Temperature Distribution

For this second case, the temperature distribution is assumed to vary according to linear law. It is represented as,

$$T(z) = \frac{T_{cnt} - T_m}{h}\left(z + \frac{h}{2}\right) + T_m \tag{19}$$

5.2.2 Linear Material Property Variation

Initially, the volume fraction of CNT is assumed to vary according to linear law.

$$V_{cnt} = \left(1 - \frac{2z}{h}\right)V_{cnt}^*$$

Here, V_{cnt}^* depends on density and mass fractions of both matrix and CNT. According to this law, the material properties can be,

$$E(z) = E_m + E_{cm}\left(1 - \frac{2z}{h}\right)V_{cnt}^*$$
$$k(z) = k_m + k_{cm}\left(1 - \frac{2z}{h}\right)V_{cnt}^* \tag{20}$$
$$\alpha(z) = \alpha_m + \alpha_{cm}\left(1 - \frac{2z}{h}\right)V_{cnt}^*$$

Using *equation (19)* and *(20)* in *equation (15)* and *(16),* the expressions for final stresses and strains are as given in *eq. (18)* The values of constants C_1, C_2 and C_3 for this case are given as

$$I_0 = \int_{-h/2}^{h/2} E_{cm}\left(1 - \frac{2z}{h}\right)V_c^* dz, \qquad I_{0T} = \int_{-h/2}^{h/2} E_{cm}\alpha_{cm}\left(1 - \frac{2z}{h}\right)^2 V_c^{*2} T(z)dz,$$

$$I_1 = \int_{-h/2}^{h/2} zE_{cm}\left(1-\frac{2z}{h}\right)V_c^* dz, \qquad I_{1T} = \int_{-h/2}^{h/2} zE_{cm}\alpha_{cm}\left(1-\frac{2z}{h}\right)^2 V_c^{*^2} T(z)dz,$$

$$I_2 = \int_{-h/2}^{h/2} z^2 E_{cm}\left(1-\frac{2z}{h}\right)V_c^* dz, \qquad I_{2T} = \int_{-h/2}^{h/2} z\alpha_{cm}\left(1-\frac{2z}{h}\right)V_c^* T(z)dz$$

5.2.3 Power Law Material Distribution

In this case the temperature distribution is assumed to vary linearly along the thickness, as per given in *equation (19)*. The volume fraction is assumed to vary as,

$$V_c = \left(\frac{z}{h}+0.5\right)^n$$

Here n represents the power law index which varies for different materials. Based on this, the required material properties will be,

$$\begin{aligned} E(z) &= E_m + E_{cm}\left(\frac{z}{h}+0.5\right)^n \\ k(z) &= k_m + k_{cm}\left(\frac{z}{h}+0.5\right)^n \\ \alpha(z) &= \alpha_m + \alpha_{cm}\left(\frac{z}{h}+0.5\right)^n \end{aligned} \qquad (21)$$

The same procedure is carried out for this case as carried out in previous case. Using *equations (19)* and *(21)* in *(15)* and *(16)*, the final expressions for stresses and strains as like in *equation (18)* can be obtained. The values of constants C_1, C_2 and C_3 for this case are,

$$\begin{aligned} I_0 &= \int_{-h/2}^{h/2} E_{cm}\left(\frac{z}{h}+0.5\right)^k dz, \qquad I_{0T} = \int_{-h/2}^{h/2} E_{cm}\alpha_{cm}\left(\frac{z}{h}+0.5\right)^{2k} T(z)dz, \\ I_1 &= \int_{-h/2}^{h/2} zE_{cm}\left(\frac{z}{h}+0.5\right)^k dz, \qquad I_{1T} = \int_{-h/2}^{h/2} zE_{cm}\alpha_{cm}\left(\frac{z}{h}+0.5\right)^{2k} T(z)dz, \\ I_2 &= \int_{-h/2}^{h/2} z^2 E_{cm}\left(\frac{z}{h}+0.5\right)^k dz, \qquad I_{2T} = \int_{-h/2}^{h/2} z\alpha_{cm}\left(\frac{z}{h}+0.5\right)^k T(z)dz \end{aligned} \qquad (22)$$

B] FINTITE DIFFERENCE METHOD FOR TEMPERATURE DISTRIBUTION

5.3 FINITE DIFFERENCE METHOD

This method is adopted to calculate temperature distribution along the thickness. Initially, temperature dependant material properties are assumed according to polynomial series as given by *equation (23)*,

$$P = P_0\left(P_{-1}T^{-1} + 1 + P_1T + P_2T^2 + P_3T^3\right) \tag{23}$$

where, P_0, P_{-1}, P_1, P_2 and P_3 are known as coefficients of temperature. These constants have different values for different materials for fixed temperature range. Now, according to One-dimensional Fourier equation of heat conduction

$$\frac{d}{dx}\left[k(z)\frac{dT}{dx}\right] = 0 \tag{24}$$

where, *k* is thermal conductivity and *T* is temperature. The boundary conditions in this case are as follows,

$$T = T_m \quad at \quad z = -h/2$$
$$T = T_{cnt} \quad at \quad z = h/2$$

Equation (24) is solved by using *equation (23)* and applying boundary conditions; the solution is given as,

$$T(z) = T_m + (T_{cnt} - T_m)\eta(z) \tag{25}$$

where,

$$\eta(z) = \frac{1}{C}\left[\left(\frac{2z+h}{2h}\right) - \frac{K_{cm}}{(k+1)K_m}\left(\frac{2z+h}{2h}\right)^{k+1} + \frac{K_{cm}^2}{(k+1)K_m^2}\left(\frac{2z+h}{2h}\right)^{2k+1} - \frac{K_{cm}^3}{(k+1)K_m^3}\left(\frac{2z+h}{2h}\right)^{3k+1} + \frac{K_{cm}^4}{(k+1)K_m^4}\left(\frac{2z+h}{2h}\right)^{4k+1} - \frac{K_{cm}^5}{(k+1)K_m^5}\left(\frac{2z+h}{2h}\right)^{5k+1}\right]$$

$$C = 1 - \frac{K_{cm}}{(k+1)K_m} + \frac{K_{cm}^2}{(k+1)K_m^2} - \frac{K_{cm}^2}{(k+1)K_m^2} + \frac{K_{cm}^4}{(k+1)K_m^4} - \frac{K_{cm}^5}{(k+1)K_m^5}$$

Equation (25) gives temperature distribution along thickness and it is used in *equation (22)* and finally stresses and strains are obtained as given in *equation (18).*

5.4 Effect of CNT Orientation

Keeping all other values constant and using Young's modulus from *equation (9), equations (13)* and *(16)* are modified to evaluate the effect of CNT orientation. In this case completely oriented CNTs are considered. Change in Young's modulus will result in change in stresses. Final expression for stress and strain is obtained by using *equations (13) and (16)* in *(18)*. Same procedure is also carried out to find the effect of CNT orientation with temperature field obtained by FDM (refer *equation 25*).

5.5 RESULTS AND DISCUSSION

5.5.1 Validation of the Present Theory

A complete MATLAB code has been developed and validated with the available results in literature. Non-dimensional stresses are obtained for conventional FG Timoshenko beam and compared with available results. *Table 5.1* shows the agreement of the obtained results with that of presented by Rahini [17].

Table 5.1 Comparison of non-dimensional stresses obtained by Rahini [17] with present theory

z/h	Non-dimensional Stresses	
	Reference	Present Case
-0.5	0.85	1.1
-0.3	0.1	0.2
-0.1	-0.3	-0.4
0.1	-0.35	-0.37
0.3	0	0.02
0.5	1.0	1.0

After validation, results obtained for different cases are presented in the following subsections.

5.5.2 Numerical Analysis

The theory presented above is applied to the beam with the simply supported end conditions and rectangular cross section with width *(b) = 0.4 m*, thickness *(h) = 1 m*. The required material properties are given in *Table 5.2*.

Table 5.2 Material properties of the beam

Material	$E(GPa)$	$\rho(Kg/m^3)$	ν	$k(W/m^\circ K)$	$\alpha(/^\circ K\times10^{-6})$
SWCNT	900	2100	0.28	3500	5.1
Al_2O_3 [1]	393	3970	0.3	30.1	8.8

The shaft is divided into *10* layers along the thickness. Using above properties graph is plotted to observe the variation of Young's modulus along the thickness direction for exponential, linear and power law variation in material properties. It is as shown in *Figure 5.1*. Effect of CNT orientation on Young's modulus is shown in *Figure 5.2*. It is observed that, for increasing values of CNT volume fraction, Young's modulus is less for completely oriented CNT than aligned CNT. The temperature boundary conditions considered here are,

$$T_0 = 300^\circ K, \quad T_m = 700^\circ K, \quad T_{cnt} = 1000^\circ K$$

These boundary conditions are applied for each of the three cases. Graph is plotted to observe the temperature distribution along the thickness for exponential and linear case. It can be observed in *Figure 5.3*. Temperature distribution is also calculated by FDM for power law gradation of material properties. Comparison of this method with power law temperature distribution is shown in *Figure 5.4*. The material properties are calculated for each layer. Then the required values of constants such as $I_0, I_{0T}, I_1, I_{1T}, I_2, I_{2T}, C_1, C_2$ and C_3 are evaluated for particular cases and finally the stresses and strains are obtained. For power law distribution the power law index is taken as *5*. Same conditions are applied to find out the effect of orientation on thermal stresses and strains.

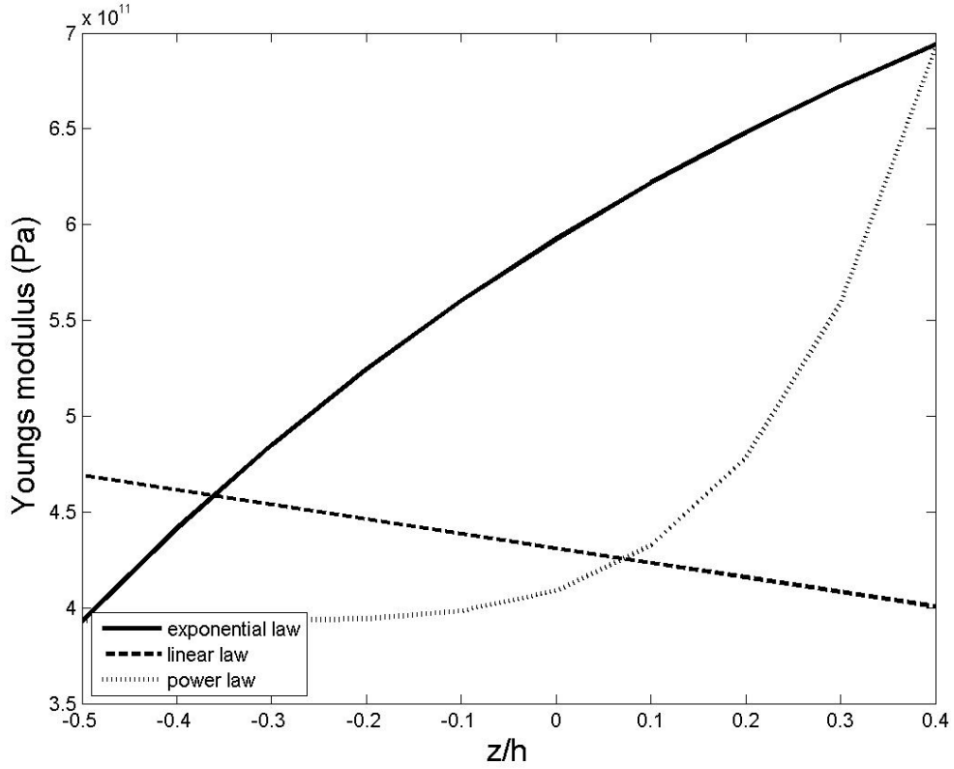

Figure 5.1 Variation of Young's modulus along the thickness for exponential, linear and power law material distribution

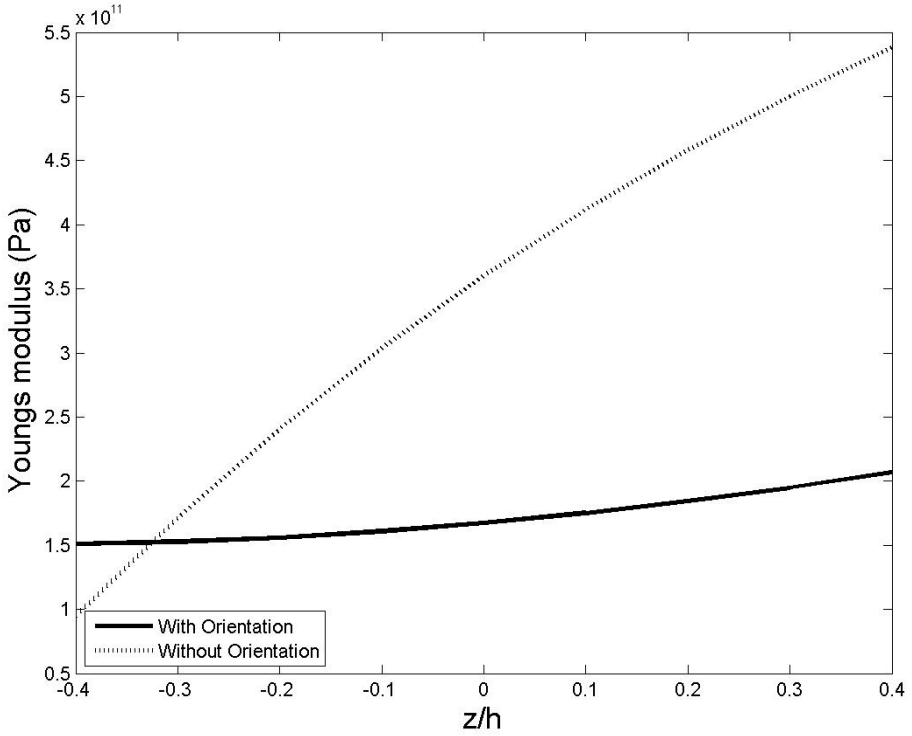

Figure 5.2 Effect of CNT orientations on Young's modulus along the thickness for exponential material distribution

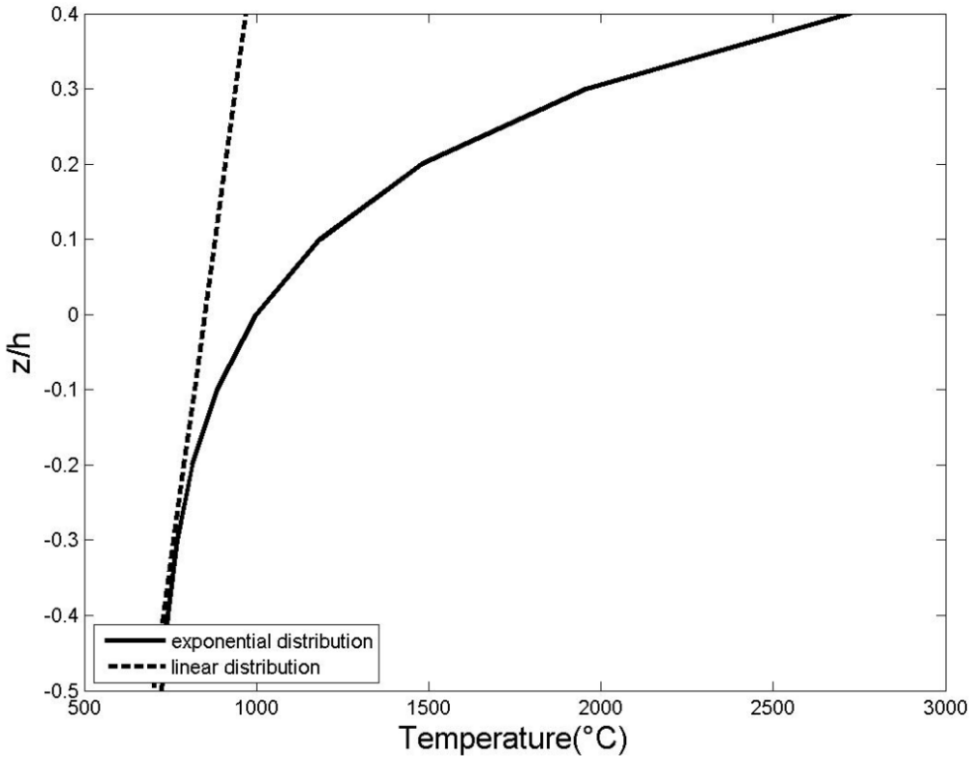

Figure 5.3 Temperature variation along the thickness according to exponential and linear distribution

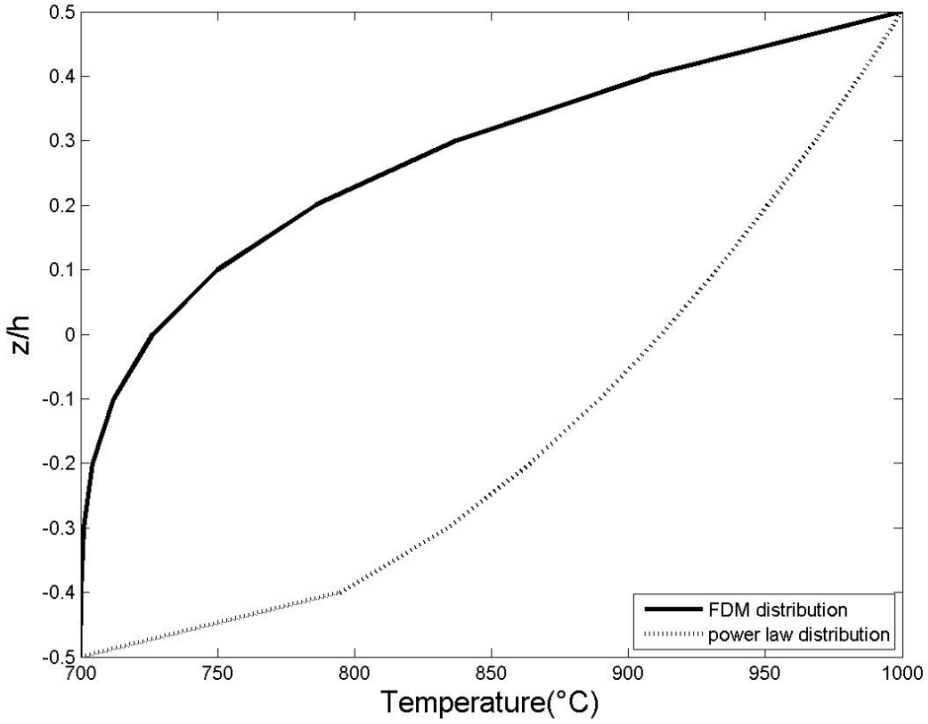

Figure 5.4 Comparison of temperature distribution along the thickness according to FDM and power law

5.5.3 Present Results

As per the formulation and numerical analysis, the results are obtained for all cases. For first case, exponential temperature distribution is applied to the beam having exponential variation in material properties and plotted graphically. For second case, the linear temperature distribution is applied to the beam having linear variation in material properties. In the end linear temperature distribution is applied for power law variation in material properties. *Figure (5.5)* and *(5.6)* shows variation of stress along the thickness of the beam and with the temperature rise respectively for each case. *Figure (5.7)* and *(5.8)* shows strain distribution along the thickness and temperature respectively for given cases.

Comparing results obtained for thickness versus stress for each case, it is observed that there is no considerable change in thermal stresses for matrix. The value of stress is almost constant because of its low thermal conductivity and less co-efficient of thermal expansion. The nature of variation of stresses will be according to the material properties i.e. for exponential variation of material properties the stress varies exponentially and so on. It is observed that for layer by layer analysis, the exponential material property variation, stresses are compressive in upper half and tensile in lower half of the beam; for linear material property variation stresses are compressive throughout; for power law material property variation stresses are tensile in upper half and compressive in lower half of the beam. Next

analysis is carried out to observe the effect of temperature on stresses and corresponding Figures show stress variation according to the temperature for different cases. Nature of variation of stresses in this case is similar to the case stress variation with thickness. At low temperatures thermal stresses are less and increases with increase in temperature which is as expected. The stresses produced in matrix part are less as compared to high CNT volume fraction part. The nature of variation of the stresses along thickness and along temperature rise is similar.

Figures showing effect on strain along the thickness for different cases yields to conclusion that as distance from the middle surface increases, the strain value also increases for first and last cases. There is no considerable change in the nature of strain variation of beam for last two cases. It is due to assumption of same temperature distribution for these cases. From the Figures relating to variation of thermal strains for corresponding temperature distribution, it can be concluded that at low temperatures strain is also less, but it goes on increasing as temperature increases. Again, it is observed that the variations of strains for linear and power law material distributions are similar. Same effect is observed on strain variation as that of stress variation when compared along the thickness and along temperature rise.

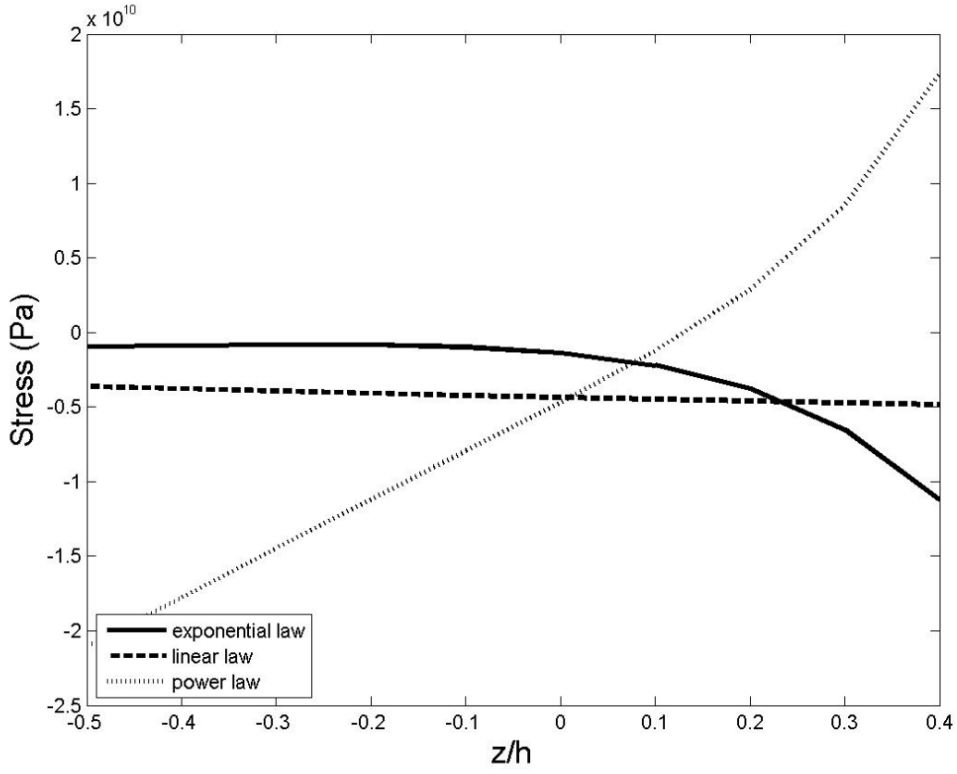

Figure 5.5 Stress distribution along the thickness for exponential material and temperature distribution, linear material distribution and linear temperature and power law material distribution

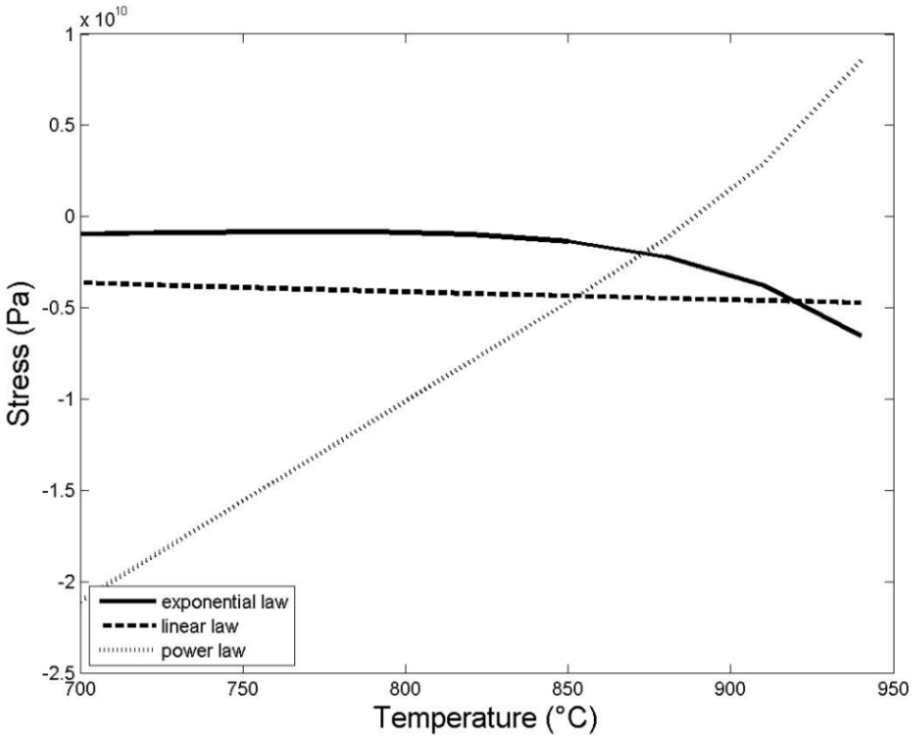

Figure 5.6 Stress distribution according to the temperature for exponential material and temperature distribution, linear material distribution and linear temperature and power law material distribution

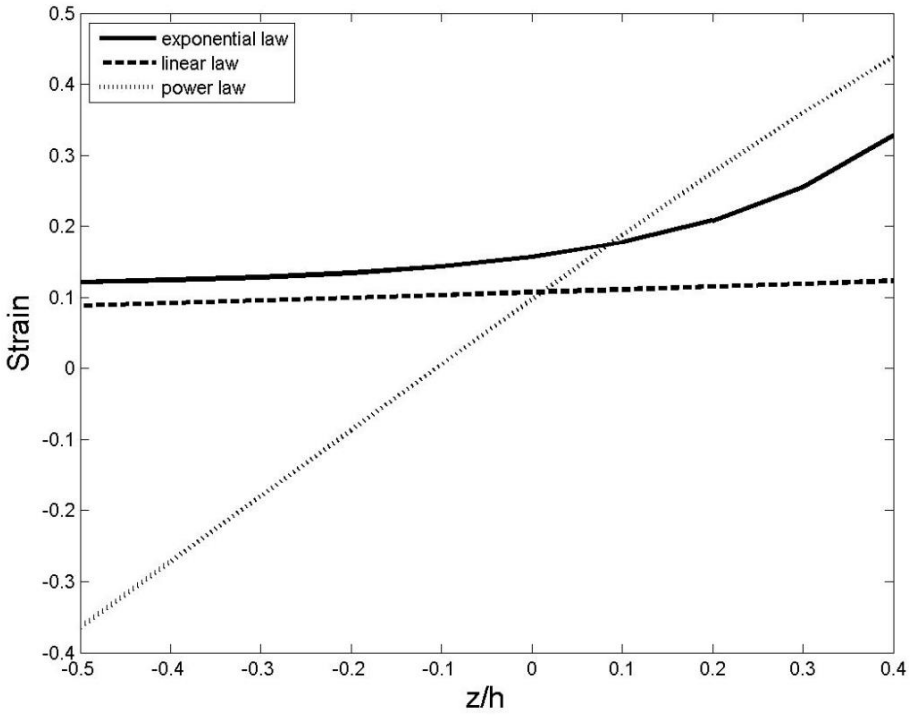

Figure 5.7 Strain variation along the thickness for exponential material and temperature distribution, linear material distribution and linear temperature and power law material distribution

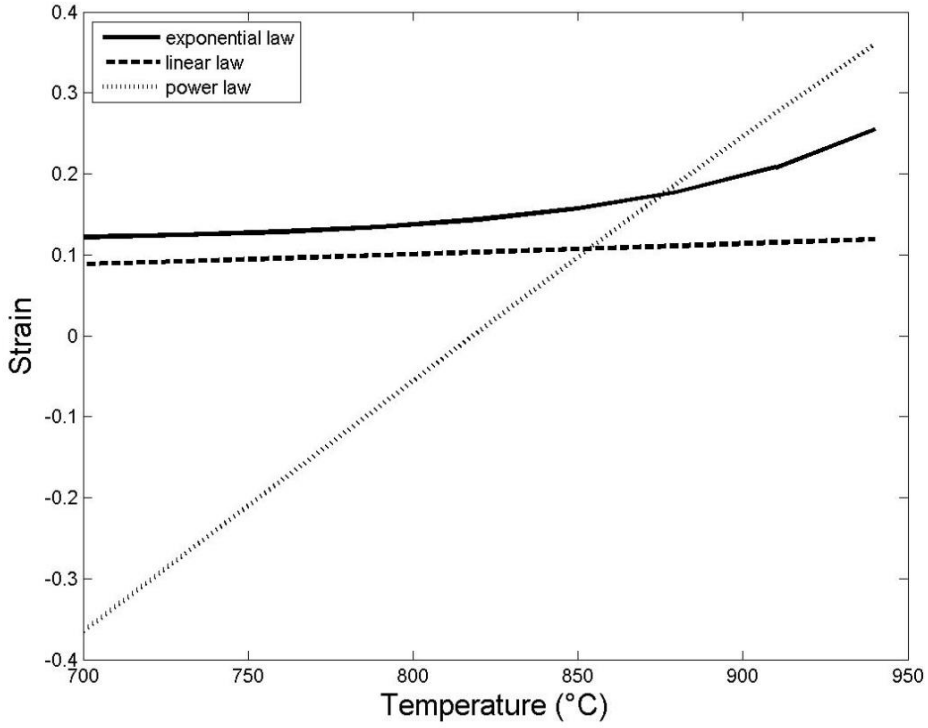

Figure 5.8 Strain variation according to the temperature for exponential material and temperature distribution, linear material distribution and linear temperature and power law material distribution

Figure (5.9-5.12) shows the effect of CNT orientation on stresses along thickness and temperature and strains along thickness and temperature. CNT orientation has significantly affected the stress distribution along the thickness as shown in *figure (5.9)*. But it is found that there is no considerable effect of orientation on stress for bottom half of the beam because it has less volume fraction of CNT. As temperature rises, the stress produced in a beam with CNT orientation considered are less than those of stresses produced in a beam with aligned CNT (as shown in *figure (5.10)*). Further, there is not significant change in strains due to CNT orientation along the thickness and temperature. This is as shown in *figure (5.11)* and *(5.12)* respectively. Change in Young's modulus has been resulted in corresponding change in stresses.

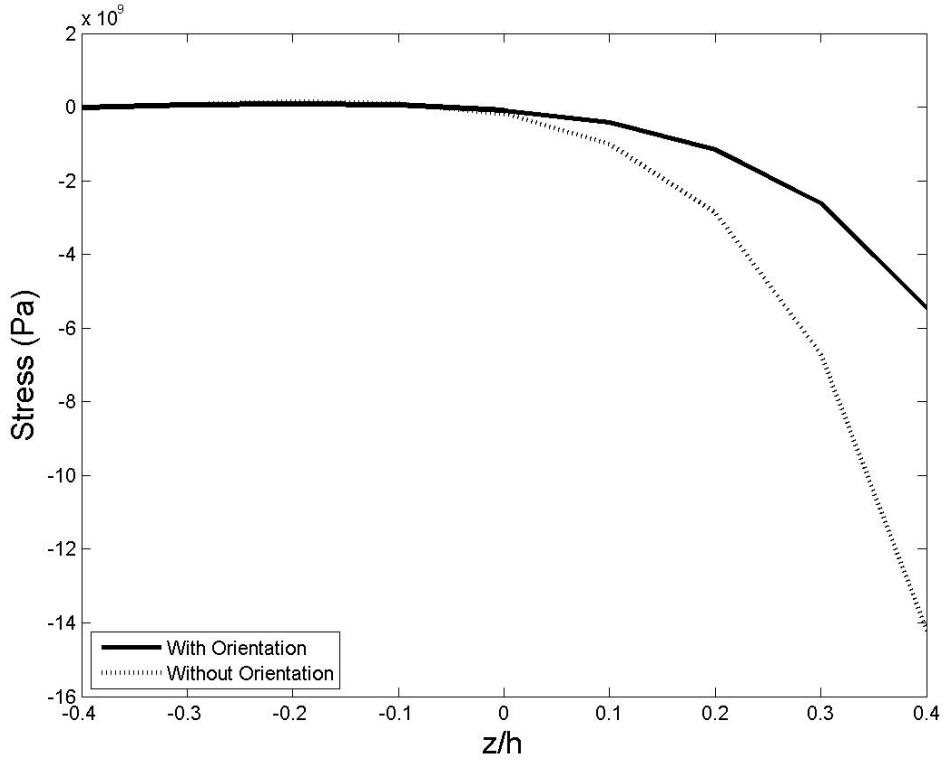

Figure 5.9 Effect of CNT orientations on stress distribution along the thickness for exponential material and temperature distribution

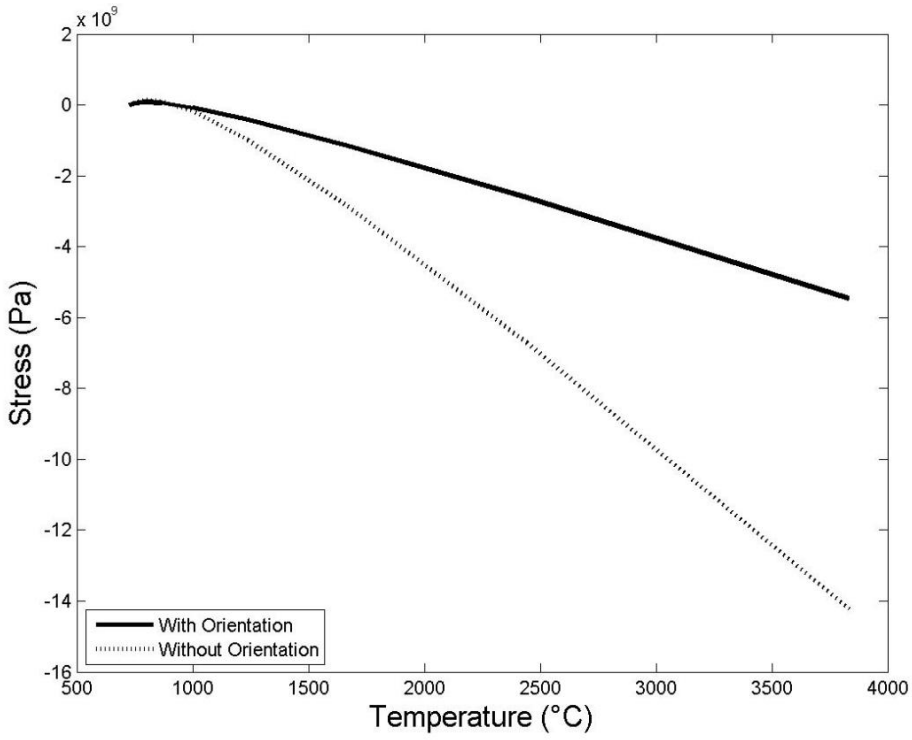

Figure 5.10 Effect of CNT orientations on stress distribution according to the temperature for exponential temperature and material distribution

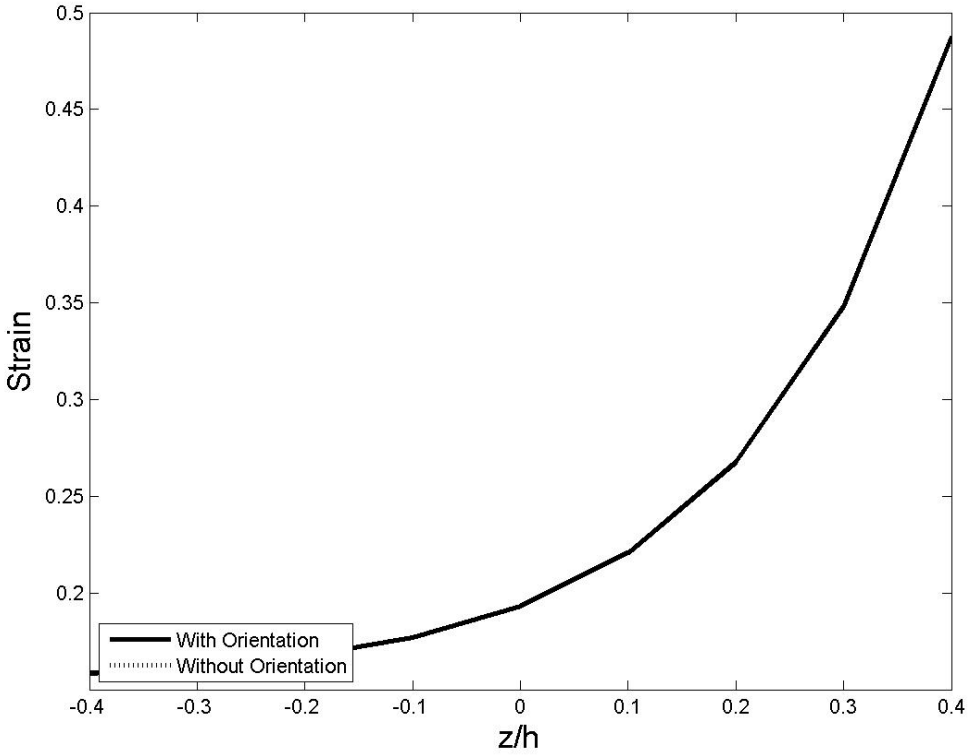

Figure 5.11 Effect of CNT orientations on strain along the thickness for exponential material and temperature distribution

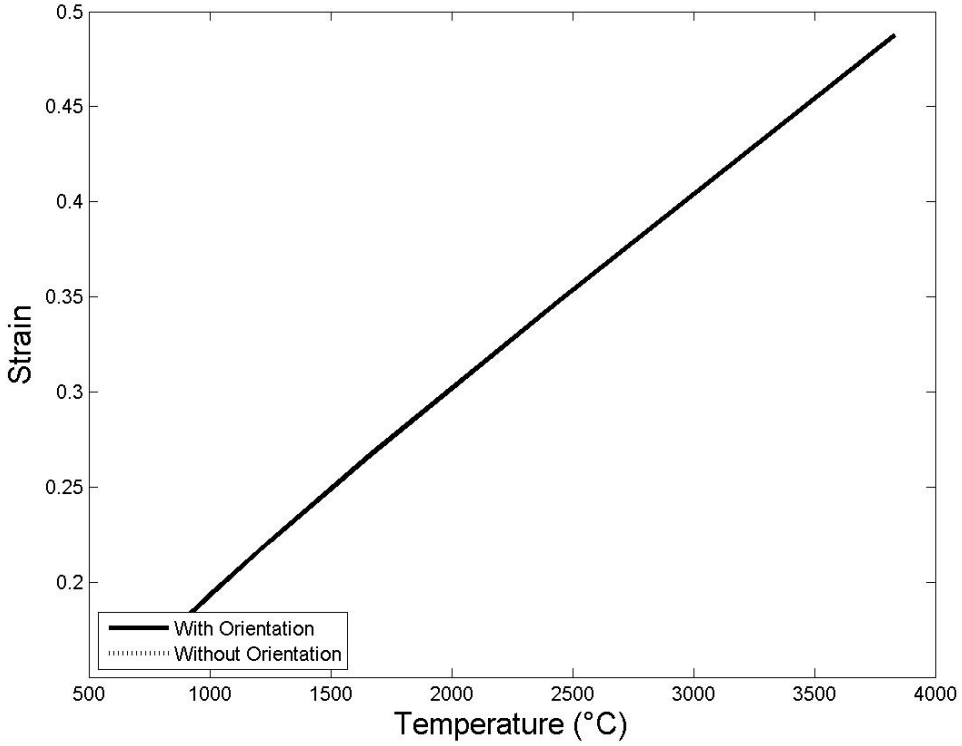

Figure 5.12 Effect of CNT orientations on strain according to the temperature distribution for exponential temperature and material distribution

Figures (5.13-5.16) shows comparison of stresses and strains developed in a beam calculated by considering the temperature distribution from FDM and simple power law. Due to these temperature distributions it is found that stress distribution is not much affected but strain distribution differs considerably. Stress variation along the thickness is as shown in *figure (5.13)* and according to temperature distribution is as shown in *figure (5.14)*. Similarly, strain distribution along the thickness and temperature is shown in *figure (5.15)* and *(5.16)* respectively. It is observed that as CNT volume fractions increases, stress and strain values increase. Although, strain decreases initially and then it goes on increasing. Similar trend is obtained for stress and strain along the temperature. As the formulae depicts, stress is directly proportional temperature, similar graph is obtained. The stress and strain variation is different for both cases, but the range of variation is same in each case.

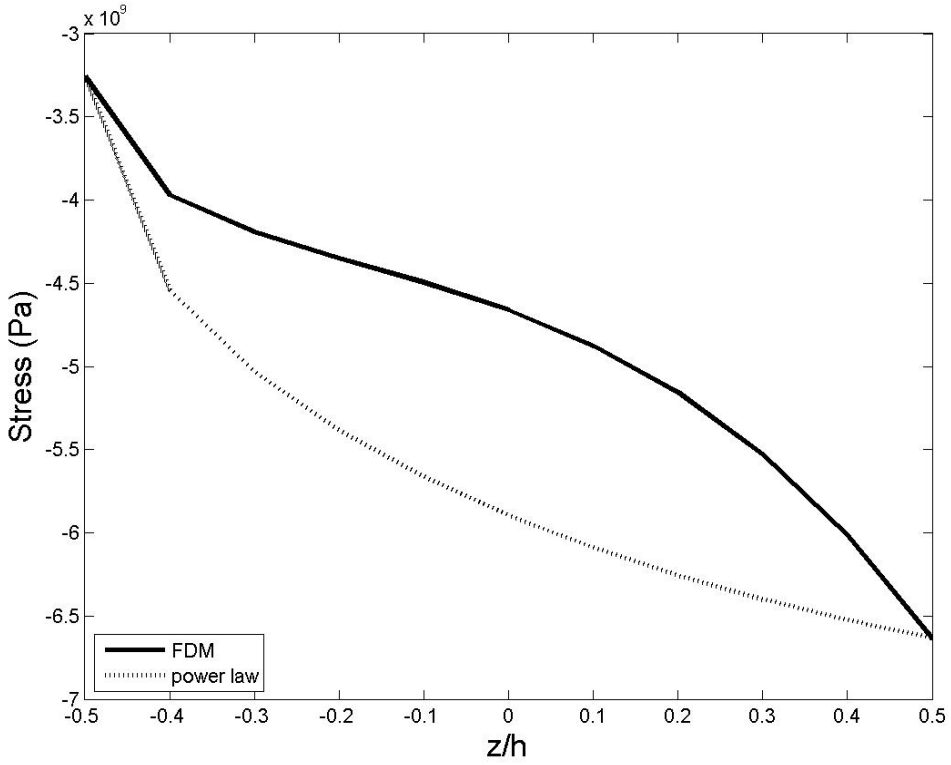

Figure 5.13 Stress distribution along the thicknness according to FDM and power law temperature distribution for power law material distribution

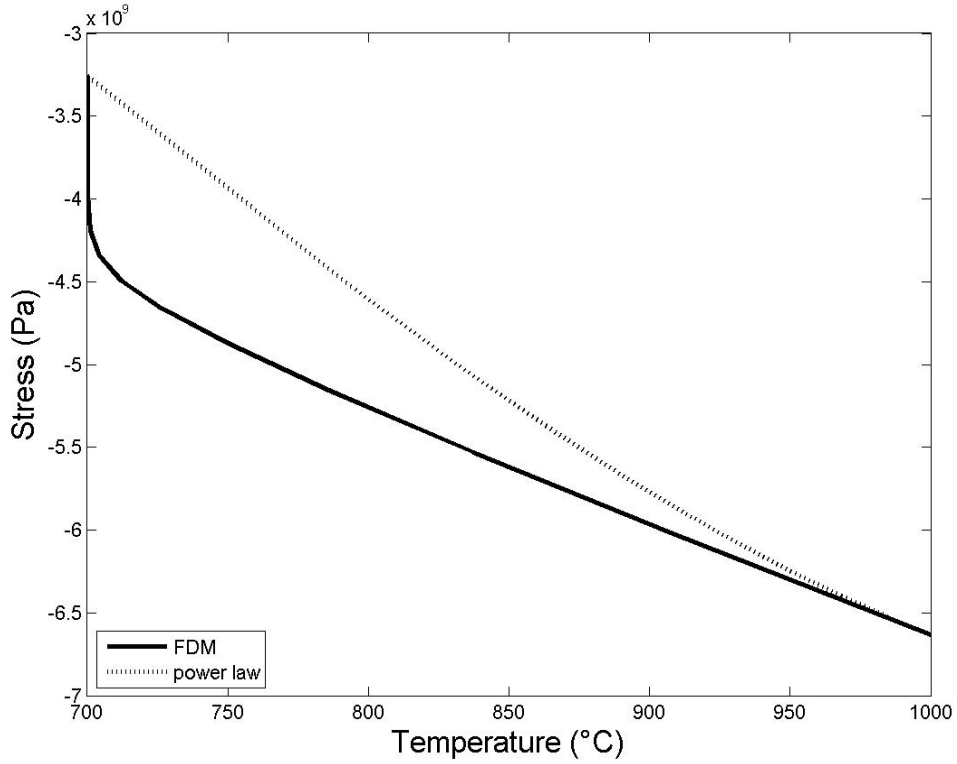

Figure 5.14 Stress distribution with the temperature according to FDM and power law temperature distribution for power law material distribution

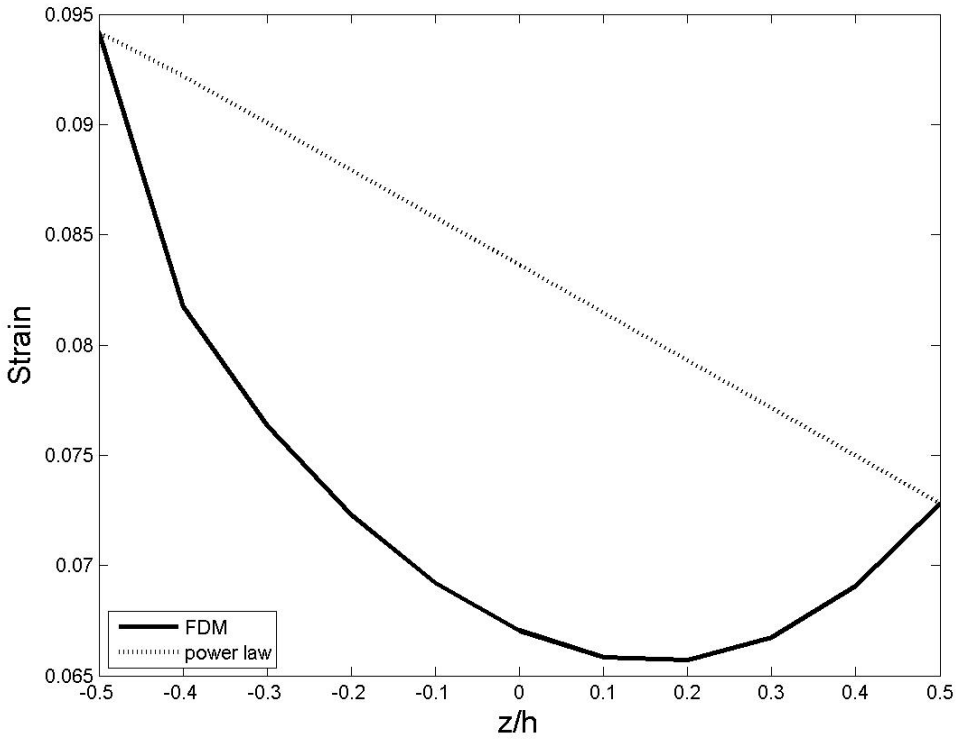

Figure 5.15 Strain variation along the thicknness according to FDM and power law temperature distribution for power law material distribution

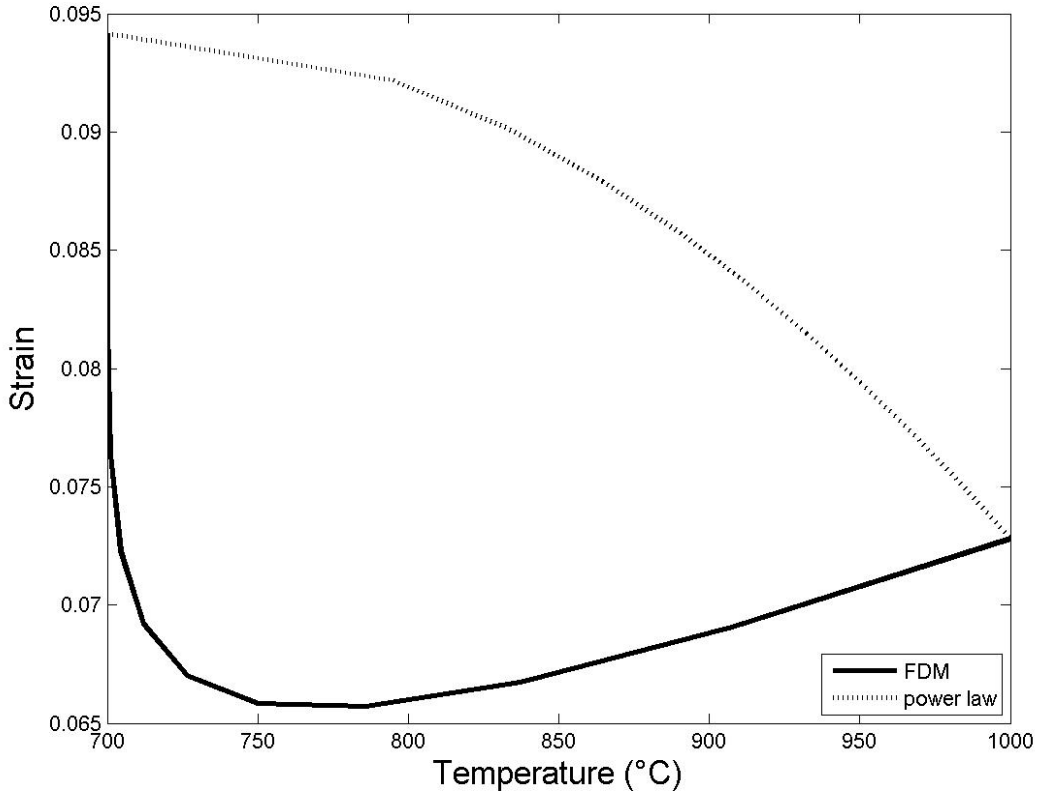

Figure 5.16 Strain variation along the temperature according to FDM and power law temperature distribution for power law material distribution

Figures (5.17-5.20) shows effect of CNT orientation on stresses and strains developed in a beam calculated by considering the temperature distribution using FDM. Reduction in Young's modulus observed previously, results in reduction in stress variation along the thickness is as shown in *figure (5.17)* and according to temperature distribution is as shown in *figure (5.18).* But, there is no effect of CNT orientation on strain distribution along the thickness and temperature is shown in *figures (5.19)* and *(5.20)* respectively. Strain variation along the thickness and according to temperature is same for both CNTs with orientation and without orientation. Similar trend of strain variation is observed as in previous case.

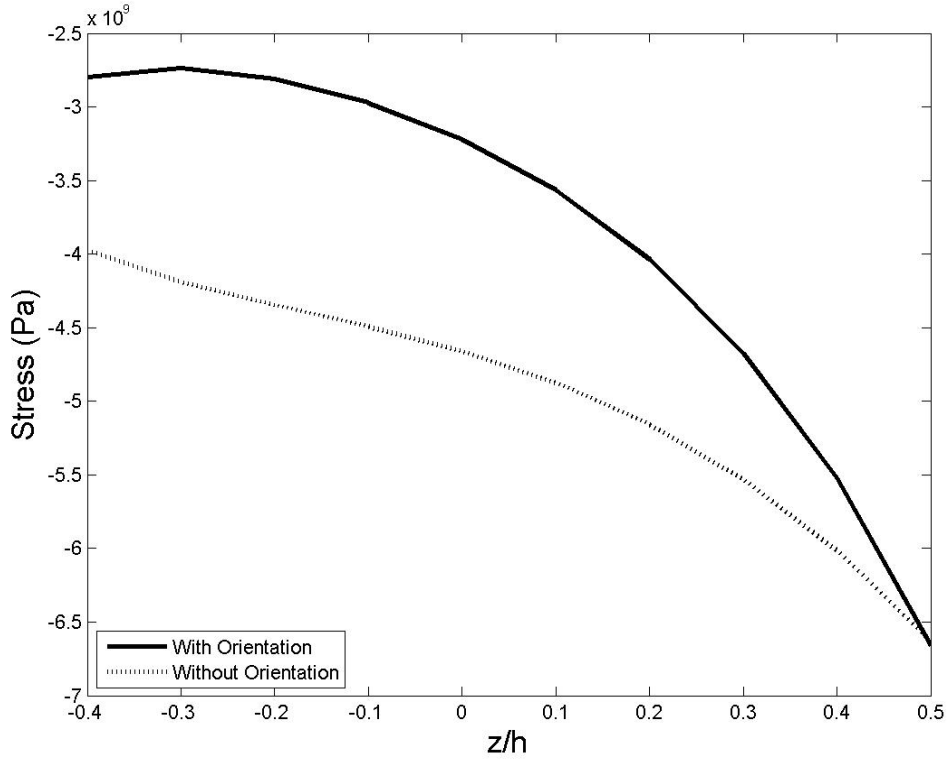

Figure 5.17 Effect of CNT orientations on stress distribution along the thickness using FDM for thermal distribution

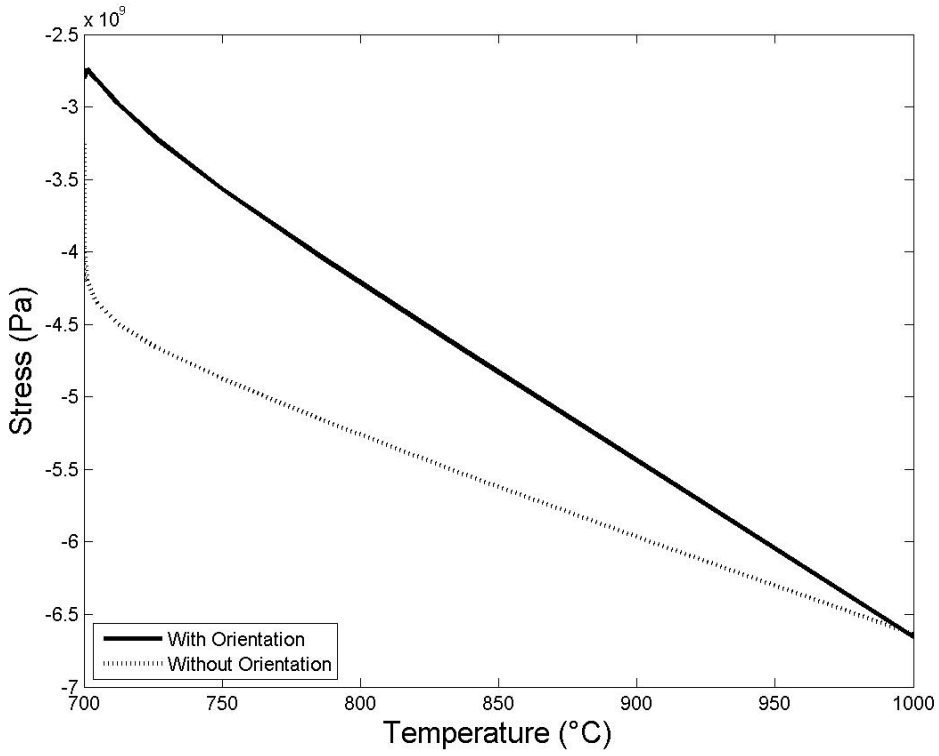

Figure 5.18 Effect of CNT orientations on stress distribution according to the temperature using FDM for thermal distribution

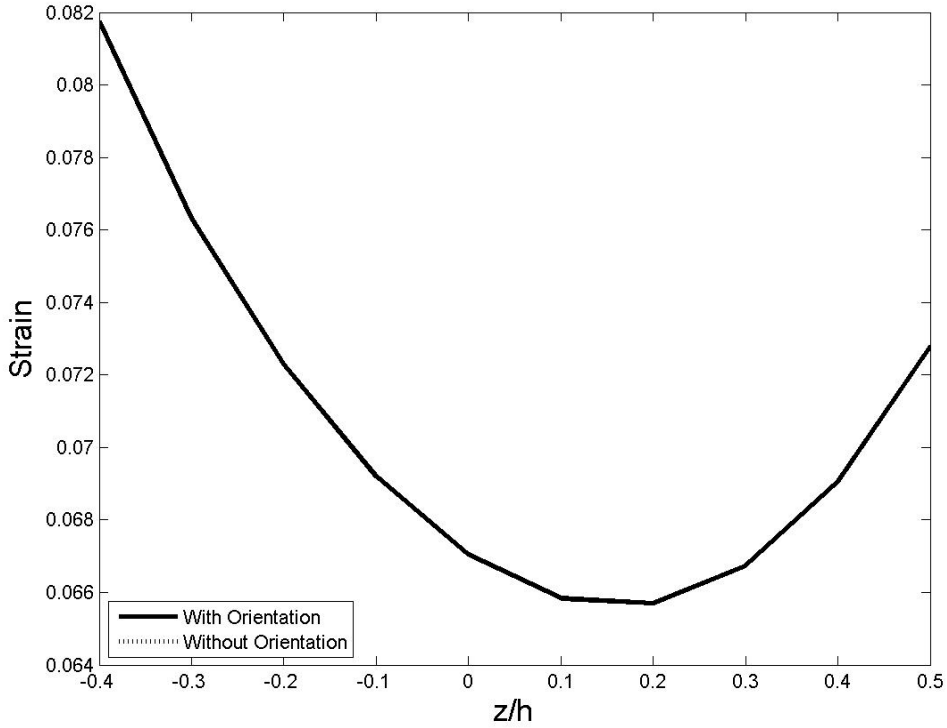

Figure 5.19 Effect of CNT orientations on strain variation along the thickness using FDM for thermal distribution

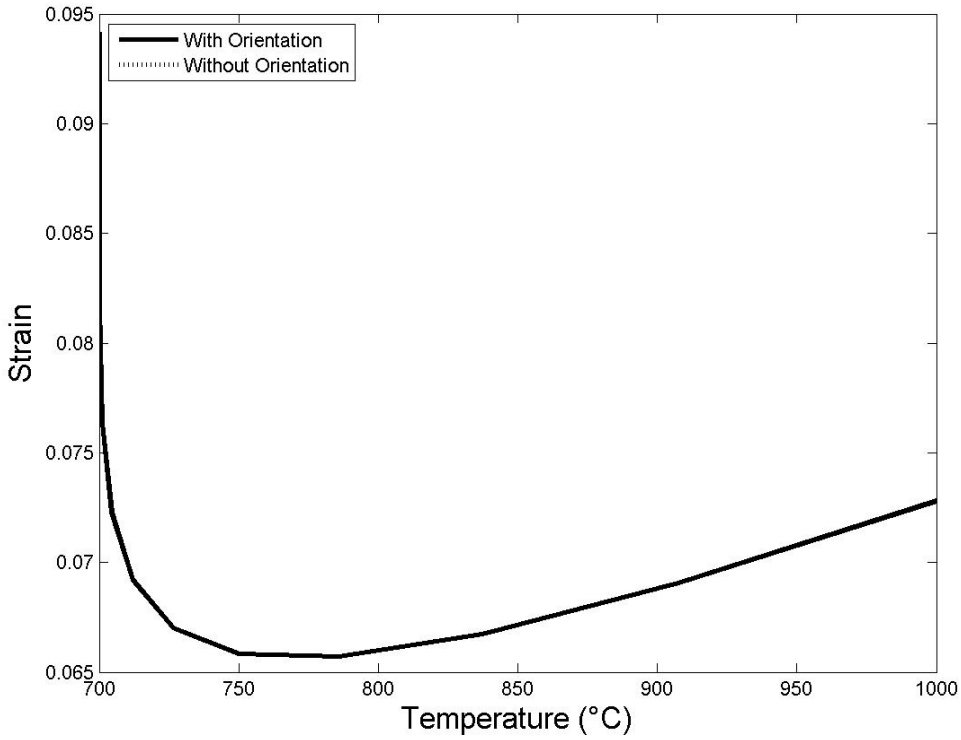

Figure 5.20 Effect of CNT orientations on strain variation according to the temperature using FDM for thermal distribution

Chapter 6

CONCLUSIONS AND FUTURE SCOPE

This chapter presents the important observations based on the total work carried out for the CNT based FG Timoshenko beam. It also gives some clues for the work that can be carried out in this area.

6.1 CONCLUSIONS

In the present work, CNT based FG Timoshenko beam has been modelled using finite element method. Firstly convergence of results has been studied and then different analyses such as static and dynamic analyses have been carried out. Non-dimensional fundamental frequencies are calculated for different volume fractions of CNT and slenderness ratio. Mode shapes and displacement diagrams are also plotted for this beam. From this analysis it can be concluded that

- As volume fraction of CNT increases, fundamental frequency also increases. The reason behind this is more volume of CNT provides more stiffness to the beam which results in higher frequencies.
- Non-dimensional fundamental frequency increases as slenderness ratio increases.
- The response of displacement versus Time shows that for increasing values of volume fraction displacement goes on reducing.
- The maximum displacement is obtained at the centre of the beam for simply supported case.

In the analysis of thermal behaviour thermal stresses and strains are evaluated numerically and plotted graphically for different cases with linear, exponential and power law temperature variation. Temperature distribution is also calculated by using FDM. That is compared with stresses and strains found by considering power law for temperature distribution. Later the effect of CNT orientation has been obtained on stresses and strains with exponential material and temperature distribution. These cases have led to following conclusion.

- The nature of variation of stresses is greatly affected by the material property variation assumed.

- The nature of variation of strains is greatly affected by the temperature distribution assumed.
- Better thermal behaviour including both stresses and strains can be obtained if the temperature distribution and material property variation are similar.
- The temperature distribution is different in both cases i.e. calculated by using FDM and power law.
- As CNT volume fraction increases, considerable changes in thermal behaviour of the beam are observed.
- Response for change in stresses and strains of matrix material is very low because of their low thermal conductivity.
- The stress and strain variation is different for FDM and power law cases but the range of variation for strains and stresses is same.
- Stress variation with temperature distribution calculated by using FDM does not vary much compared to that of calculated by power law but strain varies greatly for these two cases.
- Due to randomly oriented CNT there is reduction in Young's modulus of the beam. This reduction has led to corresponding reduction in stresses. But it is applicable for high volume fraction of CNT.
- There is no effect of CNT orientation on strain distribution either along the thickness or temperature.

So, the work presented in this paper will be useful for selecting the temperature distribution for the particular application. It will enable the design engineer to choose a particular temperature distribution so as to minimise the stresses and strains. Also, it can be concluded that FDM can be used over to other analytical methods as it is easy to implement and gives quite good results.

6.2 FUTURE SCOPE

- Vibration analysis under geometric nonlinearity
- Vibration analysis of a non-uniform CNT based FG beam
- Active vibration control of Timoshenko beam
- CNT based FG beam under thermo-mechanical loading
- Buckling analysis of non-uniform CNT based FG beam under thermal loading

REFERENCES

[1] Kiyoshi Ichikawa, "Functionally Graded Materials in the 21st Century A workshop on Trends & Forecasts", *Kluwer Academic Publishers*, pp. 1-15, 2000.

[2] Rasheedat M. Mahamood, Esther T. Akinlabi, Mukul Shukla and Sisa Pityana, "Functionally Graded Material: An Overview", *Proceedings of the World Congress on Engineering 2012*, London, U.K. Vol. III, WCE 2012, July 4 - 6 2012.

[3] J.F. Durodola and O. Attia, "Deformation and stresses in functionally graded rotating disks", *Composite Science & Technology*, vol. 60, pp. 987-995, 2000.

[4] J. Aboudi, M. J. Piranda and S. M. Arnold, "Higher Order Theory for Functionally Graded Materials", *Composites: Part B*. vol. 30, pp. 777-832, 1999.

[5] G. Giunta, D. Crisafulli, S. Belouettar and E. Carrera, "Hierarchical theories for the free vibration analysis of functionally graded beams", *Composite Structures* vol. 94, pp. 68–74, 2011.

[6] Rodney Andrews, David Jacques, Mickael Minot and Terry Rantell, "Fabrication of Carbon Multiwall Nanotube/Polymer Composites by Shear Mixing", *Macromolecular Materials and Engineering*, vol. 287, pp. 395-403, 2002.

[7] M. H. Yas and M. Heshmati, "Dynamic analysis of functionally graded nano composite beams reinforced by randomly oriented carbon nanotube under the action of moving load", *Applied Mathematical Modelling*, vol. 36, pp. 1371–1394, 2012.

[8] Amal E. Alshorbagy, M. A. Eltaher and F. F. Mahmoud, "Free vibration characteristics of a functionally graded beam by finite element method", *Applied Mathematical Modelling*, vol. 35, pp. 412–425, 2011.

[9] Liao-Liang Ke, Jie Yang and Sritawat Kitipornchai, "Nonlinear free vibration of functionally graded carbon nanotube-reinforced composite beams", Composite *Structures*, vol. 92, pp. 676–683, 2010.

[10] A. Khosrozadeh and M. A. Hajabasi, "Free vibration of embedded double-walled carbon nanotubes considering nonlinear interlayer van der Waals forces", *Applied Mathematical Modelling*, 36, pp. 997–1007, 2012.

[11] Toshiaki Natsuki, Qing-Qing Ni and Morinobu Endo, "Analysis of the vibration characteristics of double-walled carbon nanotubes", *carbon*, vol. 46, pp. 1570– 1573, 2008.

[12] M. C. Ray and R. C. Batra, "A single-walled carbon nanotube reinforced 1–3 piezoelectric composite for active control of smart structures", *Smart Material Structures* vol. 16, pp. 1936–1947, 2007.

[13] Zhen-Xin Wang and Hui-Shen shen, "Nonlinear dynamic response of nanotube-reinforced composite plates resting on elastic foundations in thermal environments", *Nonlinear Dynamics*, vol. 70, pp. 735–754, 2012.

[14] A.S. Das, M.C. Nighil, J. K. Dutt and H. Irretier, "Vibration control and stability analysis of rotor-shaft system with electromagnetic exciters", *Mechanism and Machine Theory*, vol. 43, pp. 1295–1316, 2008.

[15] A. Hossain Nezhad Shiraji, H. R. Owji and M. Rafeeyan, "Active Vibration Control of an FGM Rectangular plate using Fuzzy Logic Controllers", *ScienceDirect, Procedia Engineering*, vol. 14, pp. 3019-3026, 2011.

[16] Y. D. Kim and C. W. Lee, "Finite Element Analysis of Rotor Bearing Systems using a Modal Transformation Matrix", *Journal of Sound and Vibration*, vol. 111(3), pp. 441-456, 1986.

[17] GH. Rahini and AR. Davoodinik, "Thermal behaviour analysis of the functionally graded Timoshenko's beam", *International Journal of Engineering Science*, vol. 19, pp. 105-113, 2008.

[18] Bao-Lin Wang and Zhen-Hui Tian, "Application of finite element–finite difference method to the determination of transient temperature field in functionally graded beam", *Finite Elements in Analysis and Design*, vol. 41, pp. 335-349, 2005.

[19] Sajad Karampour, "Dimensional two steady state thermal and mechanical stresses of a Poro-FGM spherical vessel", *Procedia- Social and Behavirol Sciences*, vol. 46, pp. 4880-4885, 2012.

[20] N. Sundararajan, T. Prakash and M. Ganapathi, "Nonlinear free flexural vibrations of functionally graded rectaungular and skew plates under thermal environment", *Finite Elements in Analysis and Design*, vol. 42, pp. 152-168, 2005.

[21] Olayinka Olatunji-Ojo, A. Sandra, K. S. Boetcher and Thomas R. Cundari, "Thermal conduction analysis of layered functionally graded materials", *Computational Material Science*, vol. 54, pp. 329-335, 2012.

[22] Kyung-Su Na and Ji-Hwan Kim, "Three-dimensional thermal buckling analysis of functionally graded materials", *Composites Part B*, vol. 35, pp. 429-437, 2004.

[23] R. Javaheri and M. R. Eslami, "Thermal buckling of functionally graded plates based on higher order theory", *AIAA Journal*, vol. 40(1), pp. 162-169, 2002.

[24] T. Prakash and M. K. Singha, "Thermal post-buckling analyses of FGM skew plates", *Engineering Structures*, vol. 30, pp. 22-32, 2008.

[25] Hui-Shen Shen, "Thermal post-buckling behaviour of shear deformable FGM plates with temperature-dependent properties", *International Journal Mechanical Sciences*, vol. 49, pp. 466-478, 2007.

[26] Hui-Shen Shen, "Post-buckling analysis of axially-loaded functionally graded cylindrical shells in thermal environments", *International Journal of Solids Structures*, 39 (2002), pp. 5991-6010

[27] Esfahani, S. E., Y. Kiani, M. R. Eslami, "Non-linear Thermal Stability Analysis of Temperature Dependent FGM Beams Supported on Non-linear Hardening Elastic Foundations", *International Journal of Mechanical Sciences*, http://dx.doi.org/10.1016/j.ijmecsci.2013.01.007, 2013.

[28] J. Noack, R. Rolfes and J. Tessmer, "New layer wise theories and finite elements for efficient thermal analysis of hybrid structures", *Computers and structures*, vol. 81, pp. 2525-2538, 2003.

[29] Yiming Fu, Jianzhe Wang and Yiqi Mao, "Nonlinear analysis of buckling, free vibration and dynamic stability for the piezoelectric functionally graded beams in thermal environment", *Applied Mathematical Modelling*, vol. 36, pp. 4324-4340, 2012.

[30] K.Y. Dai, G. R. Liu, X. Han and K. M. Lim, "Thermo-mechanical analysis of functionally graded material (FGM) plates using element-free Galerkin's method", *Computers and Structures*, vol. 83, pp. 1487-1502, 2005.

[31] Hui-Shen Shen, "Nonlinear bending of functionally graded carbon nanotube-reinforced composite plates in thermal environments", *Composite Structures*, vol. 91, pp. 9-19, 2009.

[32] Hui-Shen Shen and Chen-Li Zhang, "Thermal buckling and post-buckling behaviour of functionally graded carbon nanotube-reinforced composite plates", *Material and Design*, vol. 31, pp. 3403-3411, 2010.

[33] Dong-Li Shi, Xi-Qiao Feng, Yonggang Y. Huang, Keh-Chih Hwang and Huajian Gao, "The effect of nanotube waviness and agglomeration on the elastic property of carbon nanotube reinforced composites", *Journal of Engineering Material Technology*, vol. 126, pp. 250–257, 2004.

[34] J. D. Fidelus, E. Wiesel, F.H. Gojny, K. Schulte and H. D. Wagner, "Thermo-mechanical properties of randomly oriented carbon/epoxy nano-composites", *Composites. Part A*, vol. 36, pp. 1555–1561, 2005.

[35] Gururaja Udupal, S. Shrikantha rao and K.V. Gangadharan, "Future applications of Carbon Nanotube reinforced Functionally Graded Composite Materials", *IEEE conference, Science and management*, pp. 399-404, March 30-31, 2012.

[36] Hossein Rokni, Abbas S. Milani, Rudolf J. Seethaler and Karen Stoeffler, "Improvement in dynamic properties of laminated MWCNT-polystyrene composite beams via an integrated numerical–experimental approach", *Composite Structures*, vol. 94, pp. 2538-25, 2012.

PUBLICATIONS

❖ JOURNALS

- Prasad K Inamdar and Tarapada Roy, "Effect of Temperature Distributions and Carbon Nano Tube Orientation on the Stresses Developed in a Carbon Nano Tube Based Functionally Graded Timoshenko Beam", *Mechanics based Designs of Structures and Machines journal (Tailor and Francis)*, Submitted on 30th May, 2013. **(Under Review)**
- Prasad K Inamdar and Tarapada Roy, "Thermal Analysis of a Randomly Oriented Carbon Nano Tube Reinforced Functionally Graded Timoshenko Beam using Finite Difference Method", Meccanica (Springer) **(To Be Submitted)**

❖ INTERNATIONAL CONFERENCE

- ✓ Prasad K Inamdar, D. Koteswara Rao and Tarapada Roy, "Free Vibration Analysis of Carbon Nanotube Based Functionally Graded Timoshenko Beam", *World Congress On "Frontiers of Mechanical, Aeronautical and Automobile Engineering" (WCFMAAE-2013),* Indian Institute of Technology, Delhi, New Delhi, February 2-3, 2013
- ✓ D. Koteswara Rao, Tarapada Roy, Prasad K Inamdar, Debabrata Gayen, "Finite Element Analysis of Functionally Graded Rotor Shaft Using Timoshenko Beam Theory", ICMPE Kolkata, 15th February, 2013
- ✓ Benedict Thomas, Prasad K Inamdar, Tarapada Roy and B. K. Nanda, "Finite Element Modelling and Free Vibration Analysis of Functionally Graded Nano-composite Beams Reinforced by Randomly Oriented Carbon Nanotubes ", ICMME Goa, 31st March 2013